TECHNISCHE HOGESCHOOL DELFT
AFDELING DER SCHEEPSBOUW- EN SCHEEPVAARTKUNDE
LABORATORIUM VOOR SCHEEPSHYDROMECHANICA

Rapport No. 452-P

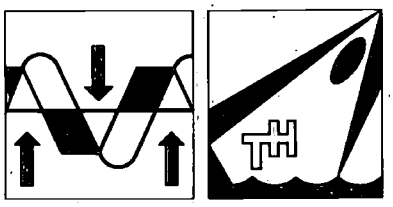

TEST RESULTS OF A SYSTEMATIC YACHT HULL SERIES

J.Gerritsma, G.Moeyes and R.Onnink

5th HISWA Symposium Yacht Architecture, november 1977

Delft University of Technology
Ship Hydromechanics Laboratory
Mekelweg 2
Delft 2208
Netherlands

august 1977

Contents:

*) Delft University of Technology,
Ship Hydromechanics Laboratory.

1. Introduction.

Systematic research on the hydrodynamic characteristics of yacht hull forms has only been carried out on a rather limited scale.
Already during the discussion of Davidson's classical paper on experimental studies of the sailing yacht, in 1936 [1], two of the discussers focussed the attention to the necessity of a systematic investigation of yacht hull forms, to give a more rational base for design methods and performance analysis. In this respect a parallel was drawn with the well-known Taylor Series, the results of which are still in use with naval architects to determine the resistance of merchant- and naval ships in the design stage [2] .
This discussion took place some forty years ago, but already at that time those concerned with yacht research and yacht design were well aware of the fact that systematic design for sailing yachts could be extremely useful to analyse the influence of hull form and sailplan variations.
The possibility to determine the performance of a yacht by varying the sail geometry and the stability of a given design, based on the results of one particular model test had been available for some time, and it was also possible to include in the analysis a variation of the yacht's size, keeping the same geometrical form.
An additional possibility, to include form variations could be considered as a useful and even necessary extension of the existing methods.
In this respect the rating of racing yachts is a special area of interest. The determination of a yacht's rating as a function of hull geometry, sail dimensions and stability is important because designers of racing yachts try to optimize hull and sails to produce an optimum combination of rating and speed potential. Rule makers aim at equal performance at equal rated length for fair competition.

There is no doubt that designers of cruising and racing yachts would benefit from the results of systematic model tests, although the problems are of such a complexity, that the full scale experiment, a "one off" will continue to play an important role in development of yacht designs.

Systematic model tests have been carried out for 12-meter yachts, because in this case the research costs for one individual design is not a very restrictive factor. Unfortunately most of the results of such tests are confidential and concern a rather extreme class of yachts.

An interesting systematic model series of yacht hulls has been presented by De Saix on the 2nd HISWA Symposium in 1971 [3] . He varied the lines of the parent model, Olin Stephens' "NY 32", to study the effect of the beam-draft ratio (5 models) and the prismatic coefficient (3 models).
De Saix remarks in his paper:

> "It is hoped the work will encourage others in the same position as the author to contribute systematic data for the use of the individual yacht designer."

Gerritsma and Moeyes published the results of a small systematic series consisting of three models with equal waterline length, breadth and rating, but with a considerable variation in the length-displacement ratio [4].
With regard to fin keels and rudders, isolated or in connection with the hull, a reasonable amount of systematic work has been carried out by De Saix [5] , Millward [6], Herreshoff and Kerwin [7], Beukelman and Keuning [8], and others.
This summary is not considered as complete, but it may serve to give an impression of the hydrodynamic research on sailing yachts, other than model testing of individual designs.

The entire problem of yacht performance is very complex and includes also the sail forces.
The combined knowledge of hull forces and sail forces can be used to simulate sailing conditions, for instance to determine the speed made good and the heel angle under given wind conditions.
Computer techniques allow the analysis of a large amount of data and consequently many combinations of hull forms and sailplans can be considered when the basic hydrodynamic and aerodynamic data are available.
To this end sail forces have to be known as a function of wind speed and apparent wind angle for the considered sail configuration. For the close-hauled condition the well known Gimcrack coefficients are commonly used.
Some forty years ago these coefficients have been derived by Davidson from full scale tests with the yacht "Gimcrack" and corresponding yacht model tests [1] . The assumption being made was that in the equilibrium condition, defined by forward speed, heel angle and leeway angle, the driving sailforce is equal in magnitude but opposite in sign with the longitudinal water resistance force. The same holds for the heeling sailforce and the sideforce, acting on the under water part of the yacht. The hydrodynamic forces can be determined from experiments with a model running in the same conditions (speed,

heel angle, leeway angle) as during full scale tests and consequently the sail-forces follow from the above mentioned equalization of sail- and hull forces. It is assumed that the sail force coefficients, derived in this way are independent of the planform of the sails.

Although the Gimcrack coefficients are restricted to the close-hauled condition, the method can be extended to other points of sailing.

A theoretical calculation of sail forces with sufficient accuracy is not yet available, although attempts have been made by Milgram [15] to investigate the influence of planform on sailforces with vortex sheet calculations. In some special cases wind tunnel measurements with model sails have been carried out [9],[10] . Systematic model experiments with a sail configuration of a cruising sloop, for all points of sailing have been carried out by Wagner and Boese [11].

These wind tunnel tests included the main sail, the working jib, genoa and spinnaker, in combination with the part of the hull above the waterline, as well as the aerodynamic forces on the hull only.

The various sail combinations were also tested without the hull.

In view of the age of the Gimcrack measurements two new determinations of sailforce coefficients have been carried out in 1974, using Davidson's method to combine model tests and full scale data. They concern the American yacht "Bay Bea" [12] and the Dutch yacht "Standfast" [13]. In the latter case the extensive model test program included the applied rudder angle, which could therefore be added to define the sailing condition to match the model and full scale results. The new data cover all points of sailing. The sailforce coefficients derived with these experiments are larger than the "Gimcrack" values, which may be due to the more efficient sailplans and the modern materials, used for sail cloth.

The experience of testing a fair number of individual yacht designs in the Delft Ship Hydromechanics Laboratory led to the conclusion that, within the time available for yacht research, much more knowledge could be obtained by testing a systematic series of yacht hulls, with variations in hull form. This series was planned to contain primarily variations of length displacement ratio, prismatic coefficient and longitudinal position of the centre of buoyancy, and should consist of approximately 27 models to cover most types of yachts. In an early stage of planning a cooperation of Delft with the Department of Ocean Engineering of the Massachusetts Institute of Technology, Boston has been established in view of their H. Irving Pratt Ocean Race

Handicapping Project. This cooperation comprises generating the lines and manufacturing polyester hulls and keels of the first 9 models by MIT; towing tank testing has been carried out by the Delft Ship Hydromechanics Laboratory. Unfortunately the funds of the Pratt-project do not permit MIT to cooperate in the testing of further models.
The test results will be used by MIT to look for fair handicap systems, while after terminating the whole series the analysis of Delft intends to provide above all the designer with basic hydrodynamic design knowledge and performance estimation methods.
In this paper the results of the first nine models are discussed. A standard performance calculation has been carried out for each of the nine models, assuming a waterline length of 10 meters, a realistic sailplan and a stability conforming the present design practice for I.O.R. designs. This exercise enables the comparison of the performance of the nine models with the rating according to the I.O.R.

2. Geometric description of the systematic series.

The main form parameters of the first nine models are given in table I, in which model 1 represents the parent form. All models have approximately the same longitudinal location of the centre of buoyancy. The prismatic coefficient has an nearly equal value for models 1 - 7, whereas model 8 has a high and model 9 a low prismatic coefficient. The relations between the various main parameters are presented in figure 1 for models 1 - 9 (black spots) as well as for thirteen models to be investigated in the near future (open circles). The lines of the nine models are shown in figure 2.
Wider, narrower, deeper and shallower models have been derived from the parent model by multiplication of coordinates with a factor which is constant for the underwater part and gradually going to 1 for the above water part of the hull. The resulting cross-sections, waterlines and buttocks were faired by computer graphics with spline cubic equations, while slight corrections of the profile ends fore and aft were introduced, when necessary, to obtain more regular and realistic forms.
These corrections cause the minor differences in LCB and prismatic as shown in table I.
Variation of the prismatic coefficient was accomplished by shifting cross-sections to obtain the desired curve of cross sectional areas belonging to the prescribed C_p and LCB.

The parent model, which resembles closely the succesful "Standfast 43" designed in 1970 by Frans Maas of Breskens, has a moderate form with regard to ratio's of main dimensions. It has clean lines, without bustles or other extreme variations in the curvature of the hull surface.
With regard to the parent model, model 2 is narrow and deep, whereas model 3 is wide and shallow, where draught is referred to the canoe body. They have the same displacement as the parent. Models 4 and 5 have a constant beam-draught ratio, but nr. 4 is lighter and nr. 5 is heavier than the parent hull. Models 6 and 7 are variations in displacement at constant length-beam ratio, thus having variations in the beam-draft ratio. Model 6 is heavier and deeper, whereas model 7 is lighter and shallower. Model 8, with the high prismatic has fuller ends and Model 9 with the low prismatic coefficient has fine end sections.

Because hull form variations were the main object of the series, all models have been tested with the same fin keel and rudder. Consequently deep- and shallow hull forms have an equal keel span, although this is not common design practice.
A NACA 63_2 - 015 airfoil section has been used for the fin keel and a NACA 0012 section for the rudder. The arrangement of keel and rudder is shown in figure 3.

The waterline length of the corresponding full scale "Standfast 43" is 10 meters, so for a first analysis of the experiments the scale factor of all models has been set to $\alpha = 6.25$ and test results have been extrapolated to 10 m waterline yachts. The main dimensions of these nine yachts and some other hull data are summarized in tables IIA and IIB. Some of the derived quantities, such as wetted surface, metacentric radius etc. are given for the canoe body as well as for the combination canoe body plus keel plus rudder.
The series of nine models is to small to derive empirical relations between the main dimensions and for instance the metacentric radius $\overline{BM}$ or the height of the centre of buoyancy above the keel $\overline{KB}$. It has to be noted that the keelpoint K is assumed to lie on the base line, which is the horizontal tangent to the canoe body.
From table IIB it may be concluded that the influence of the keel and rudder volume on the vertical position of the metacenter M is quite large. This influence should not be neglected in a calculation of the initial stability of a yacht.
The computed static stability for heel angles up to 90 degrees is given in

dimensionless form in Figure 4, where the residuary stability k (ϕ) is plotted on a base of heel angle ϕ for each of the nine models.
The definition of the dimensionless residuary stability is given by:

$$k(\phi) = \frac{\overline{MN} \sin \phi}{\overline{BM}} \qquad (1)$$

and the meaning of $\overline{MN}$ in this expression is clarified in Figure 4.
For geometric similar hull forms, which could have different dimensions, the arm of the static stability moment at a heel angle ϕ follows from:

$$\overline{GN} \sin \phi = \overline{GM} \sin \phi + k(\phi) \overline{BM} \qquad (2)$$

where $\overline{GM}$ and $\overline{BM}$ correspond to the considered dimensions of the yacht.
The relative importance of the residuary stability $\overline{MN} \sin \phi$ is shown in Figure 5a and 5b, where the stability curves of models 2 and 3 (narrow and wide) are compared, assuming realistic values for the height of the centre of gravity G. For model 2 the influence of the residuary resistance is not important, whereas for model 3 $\overline{MN} \sin \phi$ is relatively large.
It is concluded that for detailed studies of a yacht's stability the determination of the initial stability ($\overline{GM} \sin \phi$) is not sufficient. In particular for wide beam hulls the residuary stability is rather important. The effect of the yacht's own wave system is not considered in this static stability calculation.

3. Experimental set-up and test results.

3.1. Experimental set-up.

All models were constructed of GRP, corresponding to a linear scale ratio 6.25 and a waterline length of 1.6 m. This size, which implies an overall length of about 7 feet, fits the usual measuring apparatus of the Delft Ship Hydromechanics Laboratory and gives in combination with the applied turbulence stimulator an adequate guarantee for consistent test results. This turbulence stimulator consists of carburundum strips on hull, keel and rudder, which arrangement is shown in figure 6. The carburundum has a grainsize 20 and is applied on the models with a density of approximately 10 grains/cm^2.
Upright resistance tests for model speeds of 0.5 m/s - 1.8 m/s (F_n 0.13 - 0.46) are carried out twice, with a "single" and a "double"

sand strip to enable the extrapolation of the measured resistance values to zero sand strip width. It is then assumed that the extra resistance due to the sand strips varies with the speed squared and the strip width. Mean values of the resistance coefficients of the strips were determined in the middle of the tested speed range (V = 1.0 - 1.6 m/s) to avoid influence of special flow phenomena (laminar flow or wave-making).
All tests have been carried out in tank nr 2 of the Delft Ship Hydromechanics Laboratory, which has a wetted cross section of 1.22 x 2.75 m.
In view of tank blockage effects the models 1, 6 and 7 have also been tested in tank nr. 1 (wetted cross section 2.55 x 4.22 m).
All resistance values, as measured in the small tank were corrected for blockage using the method given in [14] after checking the corrections with the tank nr. 1 results.

In addition to the upright resistance tests, for each of the nine models heeled and leeway tests are carried out. Heel angles of 10, 20 and 30 degrees and leeway angles up to 10 degrees have been considered. Model speeds are chosen as 1.0, 1.2 and 1.4 m/s at 10 degrees, 1.2, 1.4 and 1.6 m/s at 20 and 30 degrees heel. With these combinations of variables all practical sailing conditions may be covered.
During the tests heel angles are the result of the side force due to leeway and forward speed and to a moment produced by a weight p to be shifted transversely over a distance t . This additional heeling moment is necessary first of all because the model is fixed sideways to measure the sideforce, and the locations where the reaction forces are measured do not correspond with the centre of effort of sailforces.
Secondly the model centre of gravity is not scaled down exactly from full scale size, which necessitates a correction for stability.
The additionally applied moment is varied in magnitude to allow for an analysis with various positions of the centre of sailforces (sail plan) and centre of gravity (stability).

3.2. Upright resistance.

For each of the nine models the residuary resistance per ton displacement of the canoe body R_R/Δ_c is given in table III as a function of Froude number $F_n = V/\sqrt{gL_{WL}}$. For this comparison only displacement of the canoe body is considered because the influence of keel and rudder on residuary (mainly wave-

making) resistance is considered to be of minor importance.
For geometric similar hull forms the residuary resistance is found from:

$$R_R = R_{R/\Delta_c} * \Delta_c \quad \text{(kgf.)} \qquad (3)$$

where: Δ_c is the displacement of the canoe body.
The corresponding speed is:

$$V = F_n * gL_{WL} \quad \text{(m/s)} \qquad (4)$$

where: $g = 9.81\ m/s^2$.

L_{WL} = nominal length of waterline in m.

To find the total resistance R_T the frictional resistance R_F is added,

$$R_T = R_R + R_F \qquad (5)$$

For yachts with separated fin keel and rudder the frictional resistance is found as the summed contributions of canoe body, keel and rudder:

$$R_F = \tfrac{1}{2}\rho V^2 (S_c C_{F_c} + S_k C_{F_k} + S_r C_{F_r}) \qquad (6)$$

where: S_c, S_k and S_r are wetted area of canoe body, keel and rudder respectively

C_{F_c}, C_{F_k} and C_{F_r} is frictional resistance coefficient for respective parts

ρ is density of water at 15° C

$= 101.87\ kgm^{-1}S^2$ for fresh water

$= 104.61\ kgm^{-1}S^2$ for salt water

The frictional resistance coefficient is calculated according to the definition by the International Towing Tank Conference 1957

$$C_F = \frac{0.75}{(\log R_n - 2)^2} \qquad (7)$$

where the Reynolds number is calculated for canoe body, keel and rudder as respectively:

$$R_{n_c} = \frac{V \times 0.7\, L_{WL}}{\nu}$$

$$R_{n_k} = \frac{V \times \overline{C}_k}{\nu} \qquad (8)$$

$$R_{n_r} = \frac{V \times \overline{C}_r}{\nu}$$

with: $\nu = 1.1413 \times 10^{6}$ for fresh water of 15^{o} C

$\nu = 1.1907 \times 10^{6}$ for salt water of 15^{o} C

$\overline{C}_k$ and $\overline{C}_r$ are the average chord length of keel respectively rudder in m.

The factor 0.7 in the definition of the Reynolds number for the canoe body allows for the particular profile and waterline shape of a yacht and gives a kind of average wetted length.
The data in table III is obtained from measurements being corrected for the effects of sand strips and tank blockage.

As an example the total and residuary resistance of model 4 are given in dimensionless form in Figure 7 to show the relative importance of the resistance components. At a Froude number $F_n = 0.35$, which is approximately the maximum speed in the close-hauled condition the frictional and residuary resistance are about equal in magnitude.

To compare the upright resistance of the hull form variations figures 8a, b, c and d give the total resistance in upright condition for a waterline length $L_{WL} = 10$ m.
Four groups are considered:
Figure 8a compares the parent model with models 2 and 3 (equal displacement, narrow and deep versus wide and shallow).
Figure 8b compares models 1, 4 and 5 (equal B_{WL}/T_c, medium, light and heavy displacement)
Figure 8c compares models 1, 6 and 7 (equal L_{WL}/B_{WL}, medium, heavy and light displacement)
Figure 8d compares models 1, 8 and 9 (medium, high and low prismatic).
The figures show the primary importance of the length-displacement ratio with regard to resistance (models 4, 5, 6 and 7), the relatively small influence of the beam-draught ratio and the beneficial effect of a high prismatic coefficient at speeds above 6 $^{3}/_{4}$ knots for the considered length of waterline.

Table III and equations 3 - 8 enable the determination of the upright resistance of geometric similar yacht forms of given dimensions.
Within the range of variation the data can be used for systematic studies of yacht hull resistance.

3.3. Sideforce and leeway.

In any asymmetrical position the hull, keel and rudder develop a sideforce due to hydrodynamic action.
The dominant parameter in this respect is the leeway angle β , but also the heel angle ϕ and the rudder angle are causing sideforces, of which the horizontal component is denoted by $F_H \cos\phi$, (see Figure 9).
Although the rudder angle is important in this respect [13] this parameter is not considered here, because the object of the systematic series is to study the influence of hull form variations only.
In Figure 10 a plot has been made of model sideforce versus leeway angle for heel angles 10,20 and 30 degrees and model speeds respectively 1.2 m/s, 1.4 m/s and 1.6 m/s (corresponding to Froude numbers: 0.30, 0.35 and 0.40).
These speeds are somewhat higher than optimal sailing speeds in the close-hauled condition, but the figures may serve to illustrate some general conclusions regarding the ability to generate sideforces for each of the nine models. However it should be remembered that all models had the same fin keel and rudder.
Figure 10 c shows that model 6 (heavy displacement, deep hull) needs approximately half the leeway angle at equal sideforce as compared with model 3 and 7. Both nr. 3 and 7 have a large beam-draught ratio. A good deal of the difference is due to the zero sideforce leeway angle, which is large for the hulls with a large beam-draught ratio. Apparently the large B_{WL} / T_c hull has a larger asymmetry when heeling. The corresponding sideforce due to the hull is directed to the leeside of the yacht in all of the considered cases.
Figure 10 shows that the slope of the lines $\frac{d(F_H \cos\phi)}{d\beta}$ increases with increasing draught of the canoe body.
The data indicate that in the considered range of leeway angles a linear relation between sideforce and leeway angle exists at constant forward speed and heel angle. Within practical limits, the sideforce varies as V^2 at constant leeway and heel angle, as suggested by Kerwin [13].

Measurements of sideforce and resistance at various leeway angles but zero

heel are carried out for all nine models at speeds corresponding to Froude numbers of 0.20 and 0.35.
Although in the ocean sailing practice sideforce is commonly associated with both leeway and heel, these tests may provide useful basic information on sideforce production.
A plot of measured sideforce versus leeway angle represents the lift curve of the complete underwaterbody. Its slope in the origin, which indicates the effectiveness of sideforce production, is given for all nine models in table IV. The values are made non-dimensional by dividing by $\frac{1}{2}\rho V^2 L_{WL}{}^2$.
In confirmation of the statements above the most effective sideforce production, e.g. the steepest sideforce curve, may be expected with the deepest draughts. The slight speed dependancy is caused by the corresponding generated wave systems.
In table IV the experimental values are compared with calculations according to a method introduced by Gerritsma [16] . This method is valid for fin keel and rudder yachts and is based on a virtual extension of keel and rudder to the waterline as shown in Figure 11, after which aerodynamic theories may be applied on both fins. The extensions are assumed to represent the contribution of the hull. A graphical comparison of experimental and calculated values in Figure 11 shows that the method gives useful predictions. The root mean square relative error of the prediction is 4.4 % and 4.5 % for Froude number .20 and .35 respectively.

3.4. Heeled and induced resistance.

In addition to the upright condition, a sailing yacht experiences an extra resistance force due to heel and sideforce. This resistance component is important as shown by the analysis of model test data. For instance at the maximum attainable close-hauled yachtspeed (approximately: $F_n = 0.35$) the frictional-, residuary- and heeled + induced resistance are roughly equal in magnitude. On other courses and forward speeds the relative importance of the various resistance components is different.
The heeled resistance can be defined as the extra resistance at zero sideforce, although as shown in Figure 10, this condition requires a leeway angle to counteract the sideforce produced by the asymmetrical immersed part of the hull. Following this definition the heeled resistance and the resistance induced by the sideforce can be distinguished in Figure 12 for the case of a thirty degrees heel angle with:

$$R_\phi - R_T = R_H + R_i \qquad (9)$$

where: R_ϕ - total resistance with heel and leeway angle

R_T - total resistance in upright position

R_H - heeled resistance at zero sideforce

R_i - induced resistance due to leeway

The highest values for the heeled and induced resistance are found for models 3 and 7 (both shallow hull forms) and the lowest values correspond with the largest draught (model 6).

The differences between the highest and the lowest values are significant in the considered case ($\phi = 30^o$, V = 1.6 m/s, model value). Apparently this is due to the differences in the effective aspect ratio of the combination of keel + rudder + underwater part of the hull, which varies from model to model due to variations in hull form.

From airfoil theory the following relation between the induced resistance and the lift is known:

$$C_{D_i} = \frac{C_L^2}{\pi AR_E} \qquad (10)$$

where: AR_E - the effective aspect ratio of the wing. For the present purpose this can be written as:

$$R_i = \frac{F_H^2}{\frac{1}{2}\rho V^2 S * C} * f(\phi) \qquad (11)$$

where: S - the total wetted surface or a representative area of hull, keel and rudder combination.

In [13] Kerwin suggested for f (ϕ):

$$f(\phi) = C_1 + C_2\phi^2 \qquad (12)$$

where C_1 and C_2 are constants to be determined from the experiments.

To show the relation between the heeled and induced resistance versus sideforce as indicated by equations (9) and (11), the extra resistance $R_\phi - R_T$ is plotted on a base of $F_H^2/\frac{1}{2}\rho V^2 S$ in Figure 12.

4. Sailing performance.

4.1. Determination of sailplan and stability.

To predict sailing performance stability and sailplan must be determined for each model in a systematic way and matched consistently to the given hull dimensions.

The following method has been chosen:

a) Hull weights, including crew and equipment, are calculated with

$$W_H = C_H . L . B_{MAX} . D$$

where: - C_H is a constant, for which a value of 65 represents current construction methods, materials and crew size
- L is length in m, taken as the average of overall length and waterline length (resp. 12.65 m and 10.00 m for all models).
- B_{MAX} is maximum breadth
- D_H is depth of the hull, which equals the constant freeboard (1.15 m) plus the draught of the canoe body,

The centre of gravity of hull weight (including crew) is assumed to be at 80% of the depth above the base line and in the centre plane of the ship, So in the stability calculations no allowance is made for asymmetric crew positions.

b) The available weight for ballast is obtained by subtracting the estimated hull weight from the given weight of displacement. It is cast as lead into the keel, assuming a specific weight of 11000 kg/m^3. Thus it fills up to a certain height and gives the position of the centre of gravity of ballast.

c) The position of the total centre of gravity is obtained by adding hull and ballast parts . Stability moments are calculated.

d) Basic proportions of the sail plan as indicated in Figure 13 are assumed. Though these assumptions are in fact arbitrary they reflect the actual design practice on a base of IOR regulations and may thus represent common yachts.

e) Maintaining the proportions mentioned under d the mast height is varied in such a way that the ratio of heeling moment to stability moment at 30° heel is equal for all ships.

This ratio is represented by:

$$SR = \frac{SA.h}{(RM)_{\phi = 30^o}} \qquad (13)$$

with: $SA = \frac{1}{2}\ I.J + \frac{1}{2}.P.E$

$h = Z_{CE} + 0.4\ .\ T_T$

where: SA: represents sail area to windward

h: represents the arm of heeling moment.

I, J, P, E are sail dimensions according to Figure 13

Z_{CE}: height centre of effort of sail area SA above the waterline

T_T: total draught

For the present analysis the value of SR has been chosen as 10. The heel angle of 30^o has been selected because this value is often encountered in conditions where stability becomes an important factcr to performance.

Results of the above calculations are shown in table V for weight and stability and in table VI for sail dimensions and derived parameters. The resulting ballast ratios (table V) have normal values. The position of the centre of gravity is in some cases probably a bit low compared to normal practice. This may be caused by the wide variations in total draught, due to the use of a standard keel under different hull shapes. This is contrary to the standard total draught stimulated by the IOR.

The obtained sail plans have normal dimensions.

It must be noted that the effective sail areas downwind and to windward, as given in table VI, are calculated different from the area SA used above, though they are linearly related to SA.

The downwind area SA_{ed} consists of mainsail and spinnaker and is estimated as:

$$SA_{ed} = 1.4.I.J + \tfrac{1}{2}.\ P.\ (E + HB) \qquad (14)$$

where: HB = standard breadth of mainsail headboard.

The sail area to windward consists of mainsail area, neglecting roach, plus the area of a standard IOR 150% genoa.

Although height and area of the rigs are selected in a fixed relation to stability moment, the sail area to wetted area and sail area to displacement ratios still vary considerably. The light models 4 and 7, with low ballast ratios and according low positions of the centre of gravity, have a small sail

area compared to wetted area.
A low stability moment due to a small breadth, like with model 2, results also in a relativelyundercanvassed boat.
Contrary, a wide hull, when combined with a normal or heavy displacement, like model 3 and 5 results in relatively large rigs.

Finally the rating of the resulting designs has been calculated, assuming an equal engine weight and position and equal propellor dimensions and immersion. From table VII it appears that the rating of this series covers a margin of abt 4 feet, which is appreciable for ships with equal length.

4.2. Downwind speed.

The downwind speed is calculated from the upright resistance tests, assuming a drag coefficient for the sails of 1.2. Furthermore it is assumed that sailing downwind does not give heel and does not necessitate a rudder angle.
The results are given in Figure 14. To show the additional influence of sail area above the resistance as shown in Figure 8, the different models are grouped in the same way.

While the resistance of models 1, 2 and 3 (Figure 8a) is nearly equal, the downwind speed differs greatly due to the difference in sail area. As said before model 2 has less sail area because its narrow beam and according low initial stability does not permit to carry more sail to windward.
The beamy model 3 is just the opposite.

A comparison of models 1, 4 and 5 shows again the important effect of sail area. Though the light displacement model 4 has less resistance than 1 and 5, its downwind speed is still lower than the others because its more strongly reduced sail area.

According to figure 14c the difference in resistance between models 1, 6 and 7, as observed in Figure 8c is apparently better compensated by sail area than the foregoing combinations. The improving performance of the light displacement yacht with increasing wind speed, and the reversed characteristics of the heavy boat may be noted.

As shown in Figures 8d and 14d the influence of prismatic coefficient is of second order, at least if otherwise hull dimensions and displacement are comparable.

However, the slightly favourable effect of a high prismatic at higher boat speed and wind velocity is noticeable from both Figures.

If downwind speed as related to resistance is compared with the sail area-wetted area and sail area-displacement ratios from table VI, it may be concluded that high ratio values favour the downwind performance. As may be obvious the sail area - wetted area ratio greatly governs the lower wind speed range, while the sail area-displacement ratio may indicate the downwind speed at higher wind speeds.

4.3. Speed-made-good to windward.

The speed-made-good to windward of all 9 models is calculated according to Davidson's method [1] , using the Gimcrack sail coefficients.
However, as a result of recent investigations [13] the Gimcrack coefficients are applied to the geometric area of mainsail and genoa, including overlap, instead of the reduced effective area proposed by Davidson. This modification takes into account the improvements in sail cloth and rig design during the last decades and gives a better prediction of heeling angle without affecting the qualities of Davidson's method.
The results of the calculations are shown in Figure 15, arranged conform Figures 8 and 14. The influence of sail area and stability on windward performance above that of hydrodynamic resistance and sideforce properties may be indicated by comparing these figures.

Figure 15a presents the characteristic differences between speed-made-good curves of a narrow and deep respectively wide and shallow hull.
At lower wind speeds, if only a moderate sideforce production is required, resistance and driving force characteristics are dominant. So in this case the beamy model 3 with its large sail area attains the highest speeds, both to windward and downwind. The narrow model 2 may still be considered as under-canvassed in these conditions.
When wind speed increases the balance between stability and heeling moment and the efficiency of sideforce production becomes more important. As discussed in paragraphs 3.3 and 3.4 the deep draught model 2 requires smaller leeway angles to generate a prescribed sideforce (Figure 10c) than the shallow model 3, and does this with much less resistance increase (Figure 11). From these hydrodynamic characteristics it may be expected that at high wind speeds model 2 is better than model 3 as shown in Figure 15a. In the case of extreme wide

and shallow hulls large drops in windward performance may occur with increasing wind speed and heel angle.
With respect to models 2 and 3 it must be remarked that in practical designs model 2 should be equipped with a somewhat smaller keel, to reduce wetted area and model 3 with a more extended keel, to improve sideforce production.

Figure 15b demonstrates that the differences which models 4 and 5 show in downwind conditions are likely retained when sailing to windward. This must be largely due to maintaining a constant breadth-draught ratio when varying displacement. This results in a comparitively low stability for the light model 4, combined with a relatively low sail area as a consequence of the design rules given in paragraph 4.1. The heavy model 5 has just opposite characteristics. Besides, the shallow draught of the light model 4 results in relatively poor sideforce and induced resistance properties (see paragraphs 3.3 and 3.4) and will therefore adversely affect the speed-made-good curve at high wind velocities. In practical designs the light displacement of model 4 might have been obtained with a somewhat wider hull and combined with a deeper keel and slightly larger sail plan.

An analysis of the differences between models 1, 6 and 7 is probably more speculative.
Though the beam of model 6 should expect a sufficiently large sail area, this is apparently not enough if related to wetted area, to obtain a light weather performance which is equivalent to models 1 and 7.
The relatively worsening qualities of model 6 and the improving qualities of model 7 at true wind speeds near 9 m/s might be attributed to the shallow respectively deep draught and consequently worse and better efficiency of sideforce production. As can be seen form Figures 10c and 12 the light, shallow draught model 7 operates at very high leeway angles and gives an appreciable resistance increase due to heel and leeway, whereas the deep model 6 demonstrates good properties within this respect.

The influence of prismatic coefficient, with otherwise comparable hull dimensions and sail plan is also demonstrated in the windward performance of models 8 and 9. In the high wind speed and consequently high boat speed range, the high prismatic model 8 shows advantages above the low prismatic model 9. This phenomenon does completely agree with the resistance curves (Figures 8d) and downwind speed (Figure 14d).

As a general conclusion it may be stated that a high sail area-wetted area ratio works advantageous in light weather, whereas at higher wind speeds a deep keel and right balance between stability moment and sail area might improve the performance to windward.

4.4. Performance with respect to rating.

For racing yachts the attainable speeds have to be related to a predetermined handicap. In most European ocean races during the 1976 and 1977 seasons the handicap consisted of multiplicating the elapsed time with a TMF (Time Multiplication Factor), which was based as follows on the IOR-rating [17] .

$$TMF = \frac{A\sqrt{R}}{1 + B\sqrt{R}}$$

where: R = rating in feet

A = 0.2424 } for yachts with rating
B = 0.0567 } above 23 feet (class I - IV)

or: A = 0.4039 } for yachts with rating
B = 0.2337 } under 23 feet (class V - VIII)

Rating R and TMF are calculated for all 9 models and given in table VII.
The rating formula intends to give an estimate of the yacht's speed potential, whereas the handicap system is constructed in such a way that the derived TMF ought to be directly proportional to speed.
Figure 16 shows the speed at standard true wind speeds of 3.5, 7.0 and 10.0 m/s versus TMF, where model 1 has been used as base boat, with suffix b.
Speed is distinguished in downwind speed, speed-made-good to windward and the average speed on a standard track parallel to the wind direction, which has to be sailed to windward and downwind.
Based on the assumption that speed and TMF should be proportional to each other, lines have been drawn through the points with the aid of the least squares fit. The root mean square of the deviation of all points with respect to this line is also shown in Figure 16 with rms. Secondly the correlation coefficient of all speed-TMF combinations is determined, based on an assumed linear relationship. The results are for all sailing conditions given in Figure 16 under r.
If it is realised that the standard way in which hull forms, keel-rudder arrangements, stability and sail plans of this series are determined might give deviations from optimal designs, and if it is furthermore realised that it is impossible to set one single handicap being equally fair in all sailing

conditions, the IOR-rating system seems to be a surprisingly good speed estimator. A root mean square error of the speed prediction which is less than 2% in most conditions may be considered very satisfactory from an engineering point of view.
Yet, racing sailors will require even less "probability" in their competition results.
From Figure 16 it appears that the IOR is especially aimed at average wind conditions, represented by the 7 m/s wind velocity. Downwind speed seems to be better predicted than speed-made-good to windward. This indicates that the IOR rates fairly well the upright hull with according resistance and the downwind sail area, but has problems in discovering all significant effects of stability and the keel-rudder configuration, when going to windward. It will indeed be difficult to imply these effects in one single formula.
All statements and conclusions above are based on calculations with yachts of equal hull length, but further strongly varying parameters. Further calculations with length as additional variable may necessitate a revision of the TMF-formula with respect to its proportionality to speed for a wider length range, but will otherwise probably confirm the conclusions above.

5. Acknowledgement.

The authors want to mention the good and fruitful cooperation with Professor J.E. Kerwin, Professor J.N. Newman and O.H. Oakley, with the Massachusetts Institute of Technology at Boston, who contributed to a great deal to the success of the reported series. Further, they are indebted to Frans Maas, Breskens, for permission to use his design as parent model, and E.G. van de Stadt & Partners for their practical advices in consistently determining stability and sail plan.
Finally, thanks go to Mrs. Joke de Jager and Piet de Heer for carefully typing this manuscript and drawing the figures.

References

[1] K.S.M. Davidson
Some experimental Studies of the Sailing Yacht.
Society of Naval Architects and Marine Engineers 1936, N.Y.

[2] D.W. Taylor
The Speed and Power of Ships, Washington 1933.

[3] P. De Saix
Systematic Model Series in the Design of the Sailing Yacht Hull.
2nd HISWA Symposium 1971, Amsterdam.

[4] J. Gerritsma, G. Moeyes
The Seakeeping Performance and Steering Properties of Sailing Yachts.
3rd HISWA Symposium 1973, Amsterdam.

[5] P. De Saix
Fin-Hull Interaction of a Sailing Yacht Model
SIT, DL, Technical Memorandum 129, 1962.

[6] A. Millward
The Design of Spade Rudders for Yachts.
University of Southampton, Report 28, 1969.

[7] H.C. Herreshoff, J.E. Kerwin
Sailing Yacht Keels.
3rd HISWA Symposium 1973, Amsterdam.

[8] W. Beukelman, J.A. Keuning
The Influence of Fin Keel Sweep Back on the Performance of Sailing Yachts.
3rd HISWA Symposium 1973, Amsterdam.

[9] C. Marchaj
Wind Tunnel Tests of a $\frac{1}{4}$ scale Dragon Rig
University of Southampton, Dept. of Aeronautics.
SUYR Paper, no. 14, 1964.

[10] H.C. Herreshoff
Hydrodynamics and Aerodynamics of the Sailing Yacht.
Society of Naval Architects and Marine Engineers 1964.

[11] B. Wagner, P. Boese
Windkanal Untersuchungen einer Segelyacht.
Schiff und Hafen 1968.

[12] J.E. Kerwin, B.W. Oppenheim, J.H. Mays
A Procedure for Sailing Performance Analysis based on Full Scale Log Entries and Towing Tank Data
M.I.T. Report no. 74-17, 1974.

[13] J. Gerritsma, G. Moeyes, J.E. Kerwin
Determination of Sail Forces based on Full Scale Measurements and Model Tests.
4th HISWA Symposium 1975, Amsterdam.

[14] Principles of Naval Architecture
Editor J.P. Comstock 1967 N.Y.

[15] J.H. Milgram
Sail Force Coefficients for Systematic Rig Variations.
SNAME Technical & Research Report R-10, 1971.

[16] J. Gerritsma
Course keeping Qualities and Motions in Waves of a Sailing Yacht.
3rd AIAA Symposium on the Aero/hydrodynamics of sailing,
California, 1971.
also:
Delft Ship Hydromechanics Laboratory,
report 200, 1968.

[17] International Offshore Rule IOR Mark III
Offshore Rating Council, IYRU.

Table I

Main form parameters.

Model nr.	L_{WL}/B_{WL}	B_{WL}/T_c	C_p	$L_{WL}/\nabla_c^{1/3}$	LCB_c %
1	3.17	3.99	0.568	4.78	-2.29
2	3.64	3.04	0.569	4.78	-2.29
3	2.76	5.35	0.565	4.78	-2.31
4	3.53	3.95	0.564	5.10	-2.32
5	2.76	3.96	0.574	4.36	-2.44
6	3.15	2.98	0.568	4.34	-2.38
7	3.17	4.95	0.562	5.14	-2,31
8	3.32	3.84	0.585	4.78	-2,37
9	3.07	4.13	0.546	4.78	-2.19

Table IIa:

Main dimensions and derived quantities

Nr	L_{OA} m	L_{WL} m	B_{MAX} m	B_{WL} m	T_C m	D m	F m	∇_C m^3	S_C m^2	A_X m^2	A_W m^2
1	12.65	10.04	3.67	3.17	0.79	1.94	1.15	9.18	25.4	1.62	21.8
2	12.65	10.04	3.21	2.76	0.91	2.06	1.15	9.18	23.9	1.62	19.1
3	12.65	10.06	4.25	3.64	0.68	1.83	1.15	9.16	27.6	1.63	25.2
4	12.65	10.06	3.32	2.85	0.72	1.87	1.15	7.55	23.0	1.34	19.8
5	12.65	10.05	4.24	3.64	0.92	2.07	1.15	12.10	29.1	2.15	25.3
6	12.65	10.00	3.66	3.17	1.06	2.21	1.15	12.24	27.5	2.16	21.9
7	12.65	10.06	3.68	3.17	0.64	1.79	1.15	7.35	24.1	1.31	21.8
8	12.65	10.15	3.54	3.05	0.79	1.94	1.15	9.18	25.4	1.57	22.1
9	12.65	10.07	3.81	3.28	0.79	1.94	1.15	9.18	25.0	1.68	21.5

	volume m^3	wetted area m^2
keel	0.639	6.01
rudder	0.055	2.15
total	0.694	8.16

Table IIb:

Main dimensions and derived quantities.

Nr	I_T m^4	I_L m^4	LCF %	LCB %	$\overline{KB}^*$ m	$\overline{BM}^*$ m	$\overline{KM}^*$ m	$\overline{KB}^{**}$ m	$\overline{BM}^{**}$ m	$\overline{KM}^{**}$ m
1	12.89	113.2	-3.32	-2.29	0.53	1.40	1.93	0.45	1.30	1.75
2	8.64	99.2	-3.31	-2.29	0.60	0.94	1.54	0.56	0.87	1.43
3	19.88	131.1	-3.30	-2.31	0.45	2.17	2.62	0.38	2.02	2.40
4	9.60	102.8	-3.30	-2.32	0.48	1.27	1.75	0.39	1.16	1.55
5	19.99	131.2	-3.32	-2.44	0.61	1.60	2.21	0.55	1.51	2.06
6	12.85	113.2	-3.34	-2.38	0.71	1.05	1.76	0.64	0.99	1.63
7	12.85	109.8	-3.29	-2.31	0.43	1.75	2.18	0.34	1.60	1.94
8	12.66	120.6	-3.43	-2.37	0.53	1.38	1.91	0.45	1.28	1.73
9	13.21	105.3	-3.07	-2.19	0.52	1.43	1.95	0.45	1.33	1.78

* canoe body

** canoe body + keel + rudder

Table III

Residuary resistance per ton hull displacement.

F_n \ nr	R_R / ∇_c kg / ton								
	1	2	3	4	5	6	7	8	9
0.127	0.12	0.05	0.10	0.20	0.17	0.14	0.29	0.21	0.16
0.153	0.29	0.19	0.32	0.37	0.24	0.28	0.47	0.41	0.34
0.178	0.50	0.40	0.59	0.69	0.37	0.46	0.74	0.68	0.58
0.203	0.82	0.70	0.92	0.97	0.58	0.76	1.12	1.01	0.90
0.229	1.26	1.13	1.40	1.43	0.93	1.19	1.66	1.44	1.31
0.254	1.94	1.69	2.12	2.09	1.43	1.83	2.36	2.11	1.86
0.267	2.36	2.05	2.57	2.50	1.84	2.18	2.84	2.57	2.24
0.280	2.79	2.52	3.19	2.98	2.30	2.72	3.25	3.16	2.66
0.292	3.38	2.97	3.85	3.56	2.84	3.20	3.73	3.88	3.12
0.305	3.99	3.50	4.47	4.20	3.37	3.72	4.35	4.64	3.67
0.318	4.61	4.16	5.10	4.75	4.16	4.35	5.23	5.33	4.35
0.330	5.30	4.99	6.01	5.56	4.92	5.07	6.27	6.16	5.23
0.343	6.38	6.24	7.30	6.92	6.07	6.27	7.53	7.31	6.45
0.356	7.99	7.99	9.20	8.81	7.91	8.02	9.05	8.78	8.33
0.369	10.51	10.45	11.70	11.19	10.26	10.57	11.35	10.85	11.04
0.381	13.55	13.79	14.96	14.55	13.83	14.21	14.43	13.62	14.71
0.394	17.89	18.52	19.15	18.76	17.95	18.85	18.32	17.25	19.51
0.407	23.04	24.46	24.26	24.07	23.70	25.07	23.21	21.75	25.25
0.419	29.31	31.39	30.48	30.38	30.40	32.66	29.23	27.21	32.09
0.432	37.05	39.42	37.86	37.79	38.89	41.27	36.15	33.67	40.01
0.445	45.88	48.31	46.43	46.21	48.10	51.58	44.03	41.24	49.18
0.458	55.45	57.33	55.89	55.51	59.21	62.55	52.74	49.60	59.73

Table IV:

Calculated and measured side force curve slopes.

Nr	T m	$Y_\beta' \times 10^5$		
		measured		calculated
		$F_n = .20$	$F_n = .35$	
1	2.16	12400	12400	12630
2	2.28	12700	12800	13654
3	2.05	11800	12300	11618
4	2.09	11400	11600	11962
5	2.28	13000	13600	13688
6	2.43	14500	15500	15118
7	2.01	10800	11200	11260
8	2.16	12800	13600	12630
9	2.16	12450	13150	12630

$$Y_\beta' = \frac{dF_H}{d\beta} \Big/ \tfrac{1}{2}\rho V^2 L_{WL}^2$$

Table V:

Weight and stability data

Nr.	BR %	Z_G m	$\overline{GM}$ m	RM at $\phi = 1^o$ kgm	RM at $\phi = 30^o$ kgm
1	47	-0.34	1.30	224	6095
2	51	-0.48	1.00	173	4915
3	42	-0.19	1.90	327	7873
4	44	-0.29	1.12	161	4376
5	49	-0.40	1.54	343	9492
6	54	-0.56	1.14	256	7026
7	40	-0.15	1.45	204	4682
8	49	-0.38	1.32	227	6223
9	45	-0.30	1.29	222	5966

BR = Ballast Ratio

Table VI:

Sail dimensions

nr	I m	J m	P m	E m	SA_{ed} m^2	SA_{eb} m^2	Z_{CE} m	$\left(\frac{SA_{ed}}{S}\right)^{\frac{1}{2}}$ *)	$\frac{SA_{ed}^{\frac{1}{2}}}{\nabla^{1/3}}$ *)
1	16.47	5.49	15.02	4.29	159.8	104.7	6.99	2.18	5.89
2	15.23	5.08	13.78	3.94	136.3	89.1	6.56	2.06	5.44
3	18.07	6.02	16.62	4.75	192.9	126.7	7.55	2.32	6.48
4	14.64	4.88	13.19	3.77	125.6	82.1	6.36	2.01	5.55
5	19.24	6.41	17.79	5.08	219.2	144.0	7.95	2.43	6.33
6	17.27	5.76	15.82	4.52	176.1	115.5	7.26	2.22	5.65
7	15.02	5.01	13.57	3.88	132.5	86.6	6.50	2.03	5.74
8	16.61	5.54	15.16	4.33	162.6	106.6	7.04	2.20	5.94
9	16.34	5.45	14.89	4.25	157.3	103.0	6.95	2.18	5.84

*) The ratios of windward sail area to wetted area and displacement are proportional to the downwind sail area ratios.

Table VII:

Rating parameters

Nr.	MR m	R ft	TMF
1	10.62	34.2	1.0646
2	10.05	33.2	1.0528
3	11.40	36.7	1.0930
4	10.09	32.5	1.0443
5	11.17	36.3	1.0886
6	10.48	34.9	1.0727
7	10.30	32.9	1.0492
8	10.73	35.6	1.0807
9	10.33	33.1	1.0516

Figures:

1. Form parameters of model series.
2. Lines of models 1 - 9.
3. Fin keel and rudder arrangement.
4. Non-dimensional residuary stability, models 1 - 9, canoe body only.
5. Stability curves models 2 and 3.
6. Turbulence stimulator.
7. Non-dimensional resistance of model 4.
8. Comparison of upright resistance (L_{WL} = 10 m)
9. Sideforce and sailforce.
10. Sideforce versus leeway (model values).
11. Calculated and measured sideforce curve slopes.
12. Heeled and induced resistance.
13. Standard sail plan design.
14. Downwind speed.
15. Speed-made-good to windward.
16. Downwind, made-good and average speed related to rating.

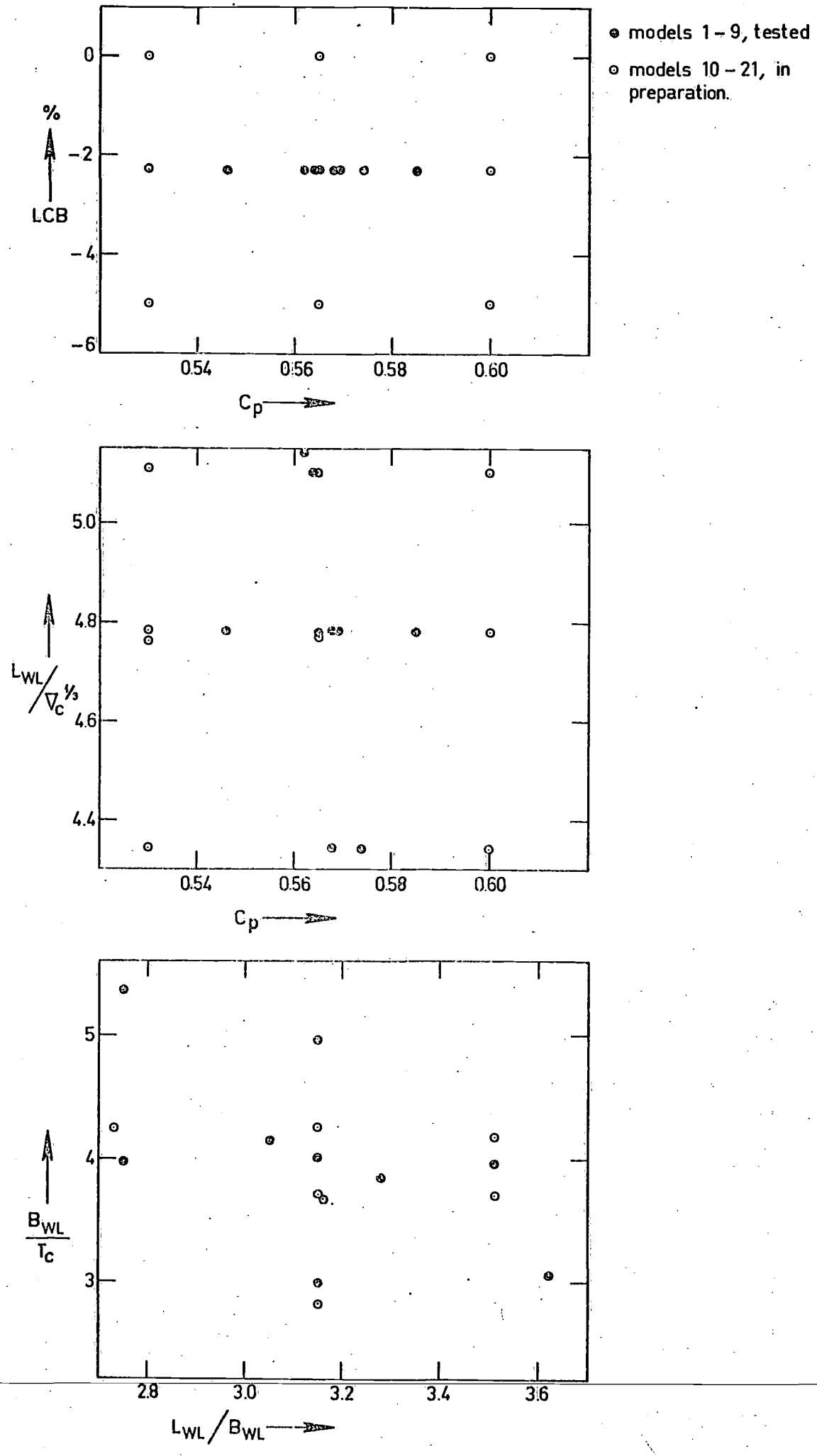

Fig. 1: Form parameters of model series.

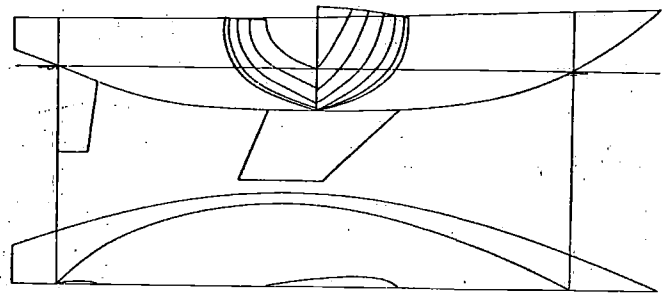

PARENT MODEL NR.1

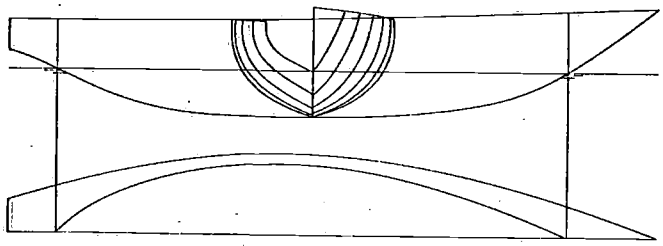

NR.2

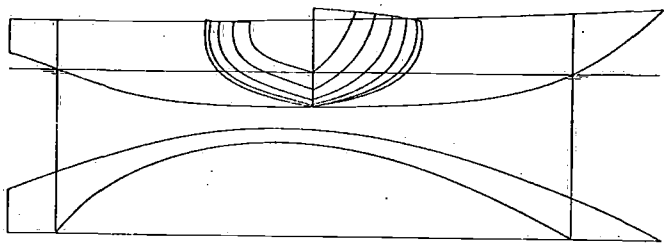

NR.3

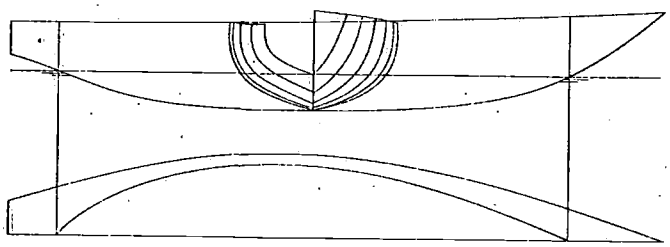

NR.4

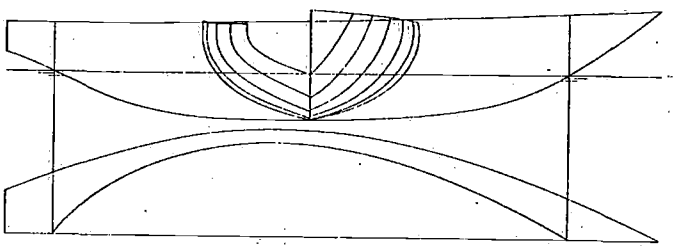

NR.5

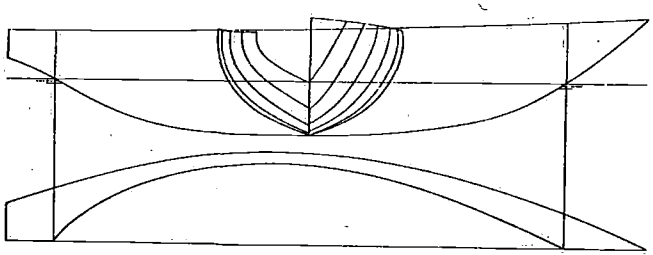

NR.6

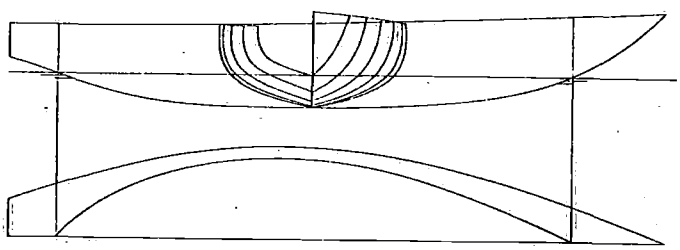

NR.7

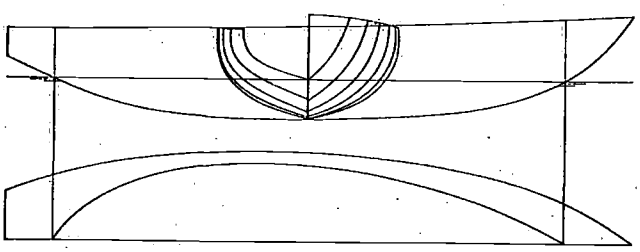

NR.8

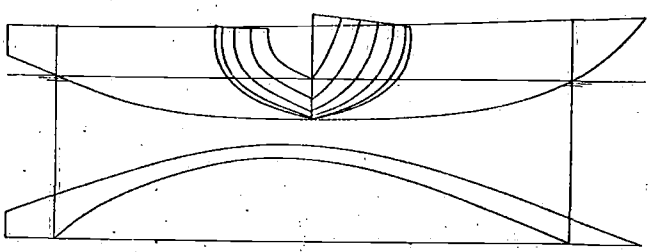

NR.9

Fig. 2: Lines of models 1 – 9.

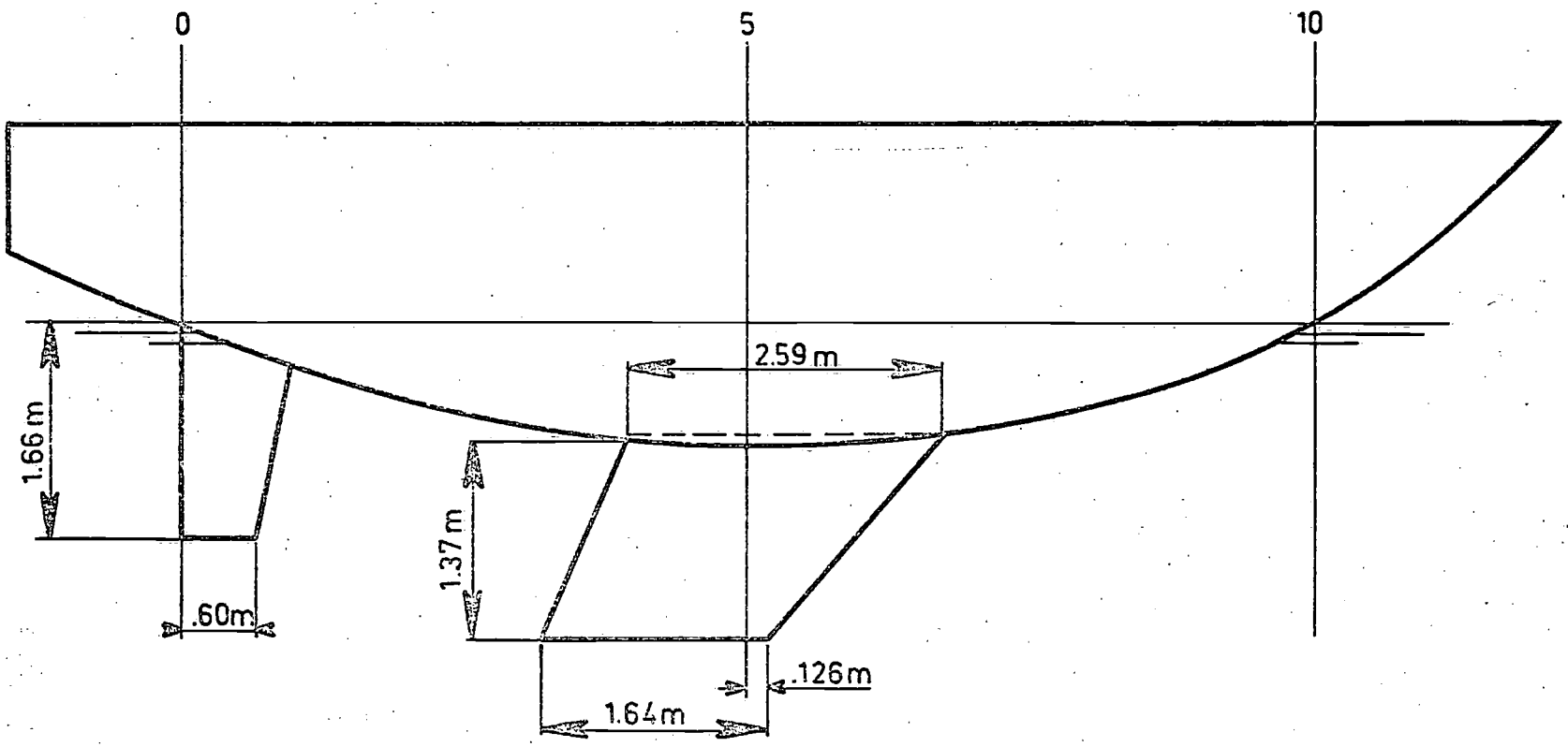

Fig. 3 : Fin keel and rudder arrangement.

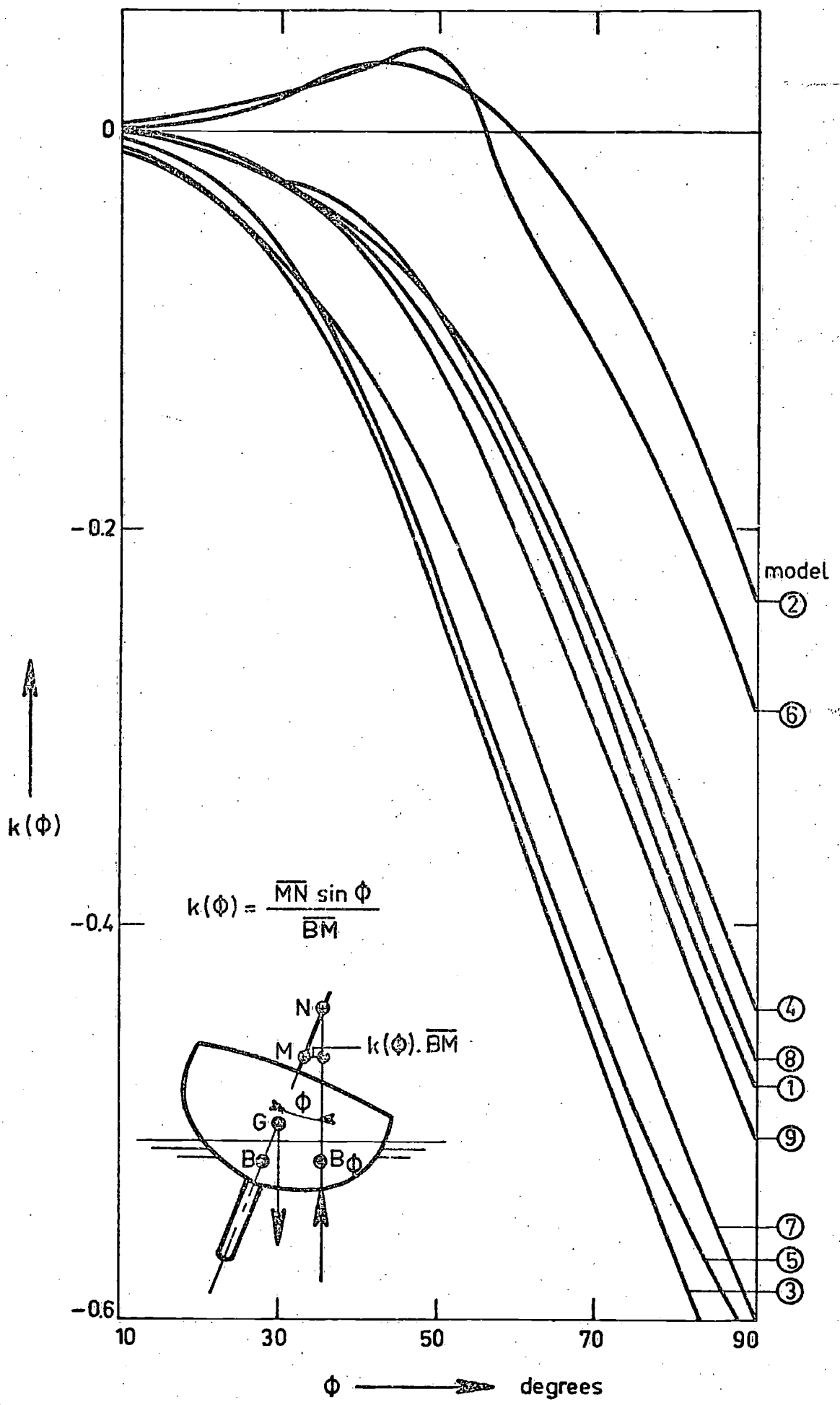

Fig. 4 : Non – dimensional residuary stability, models 1 – 9, canoe body only.

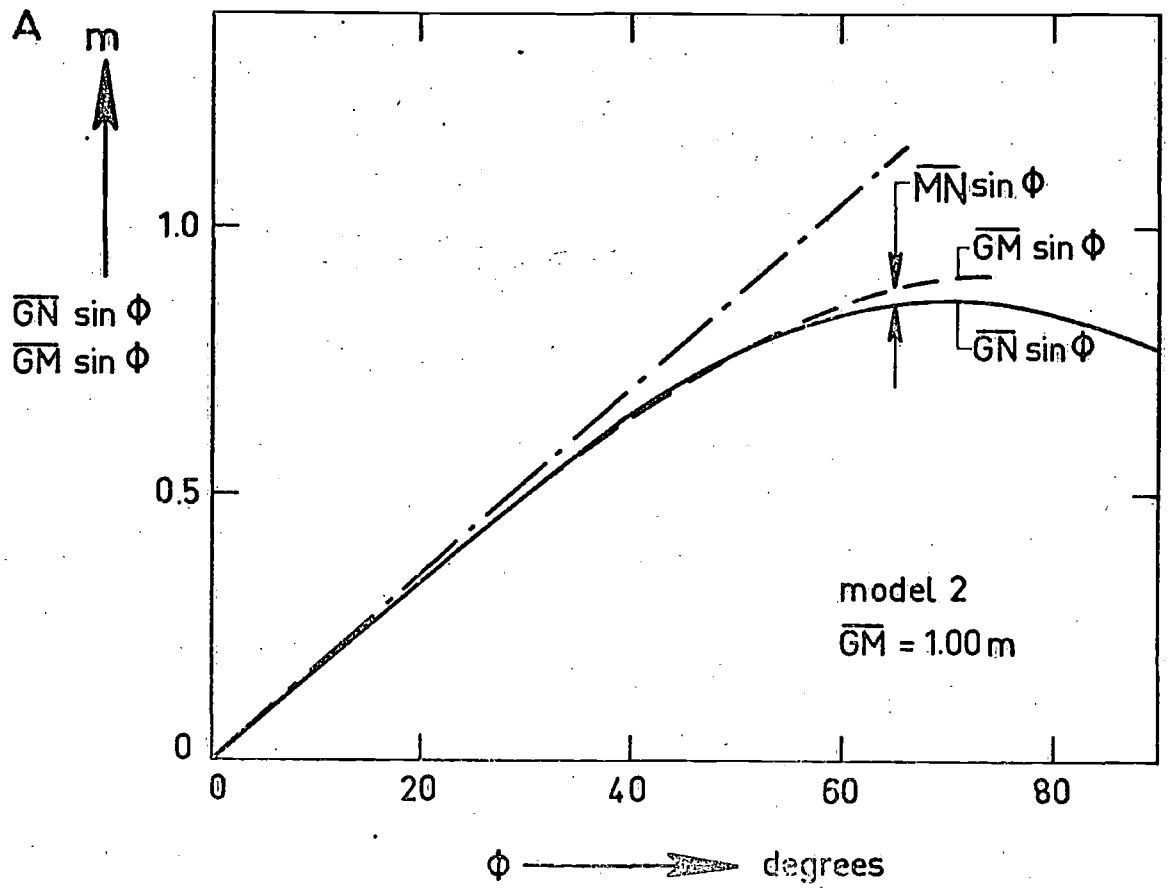

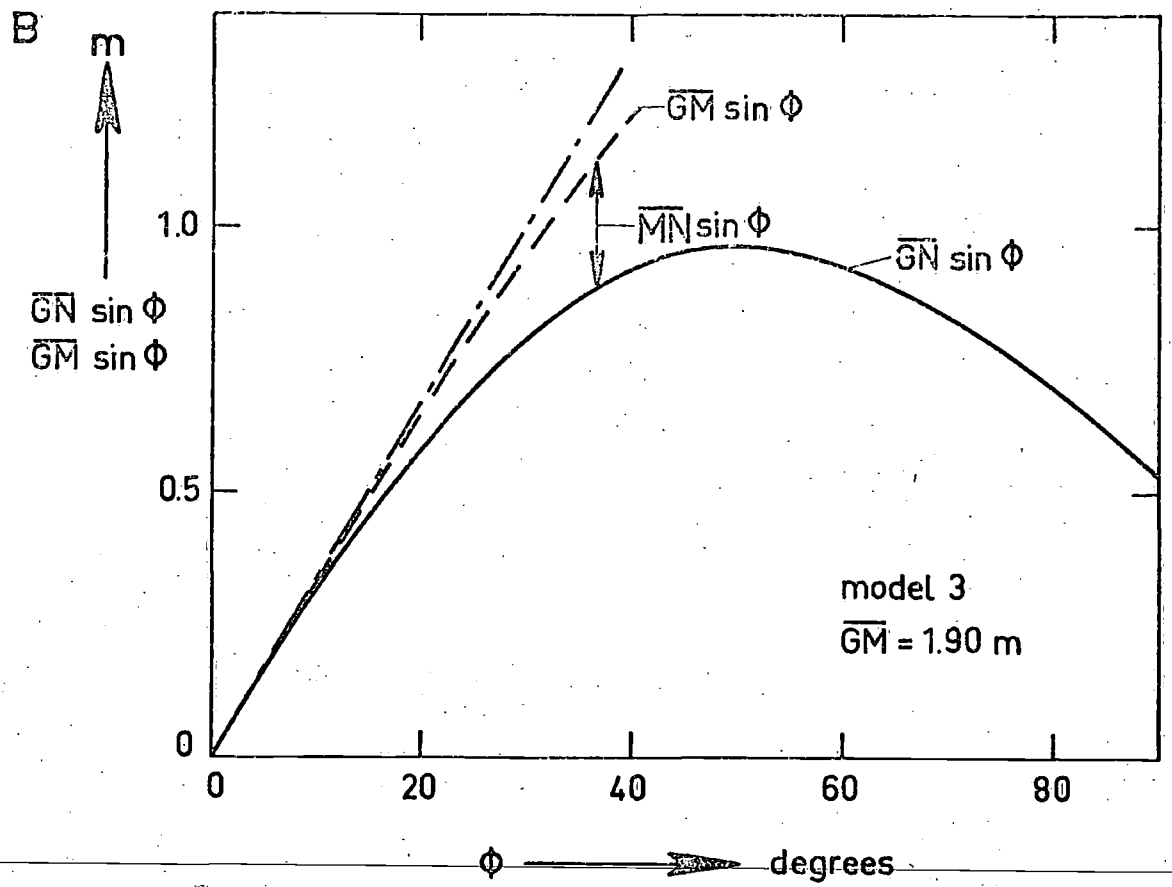

Fig.5: Stability curves models 2 and 3.

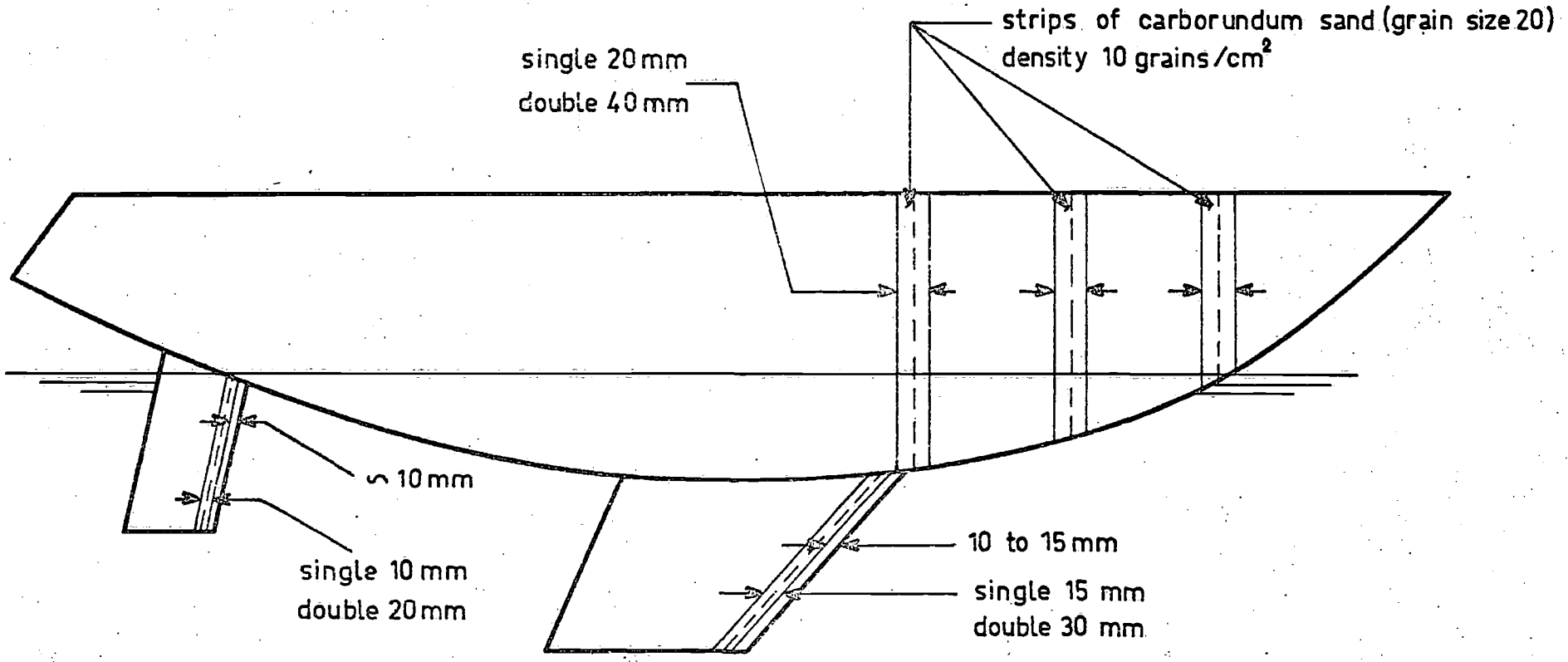

Fig. 6 : Turbulence stimulation.

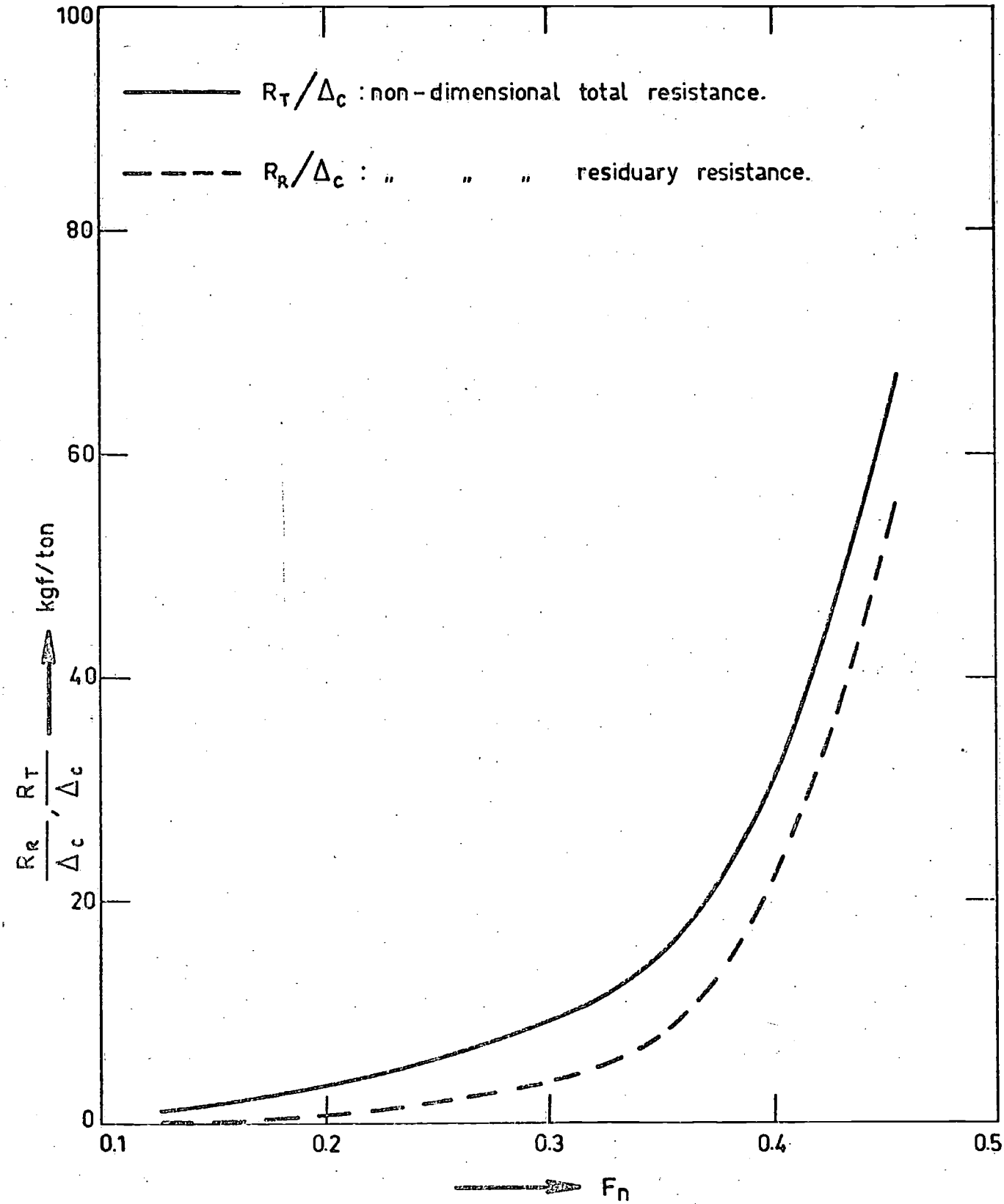

Fig. 7 : Non-dimensional resistance of model 4

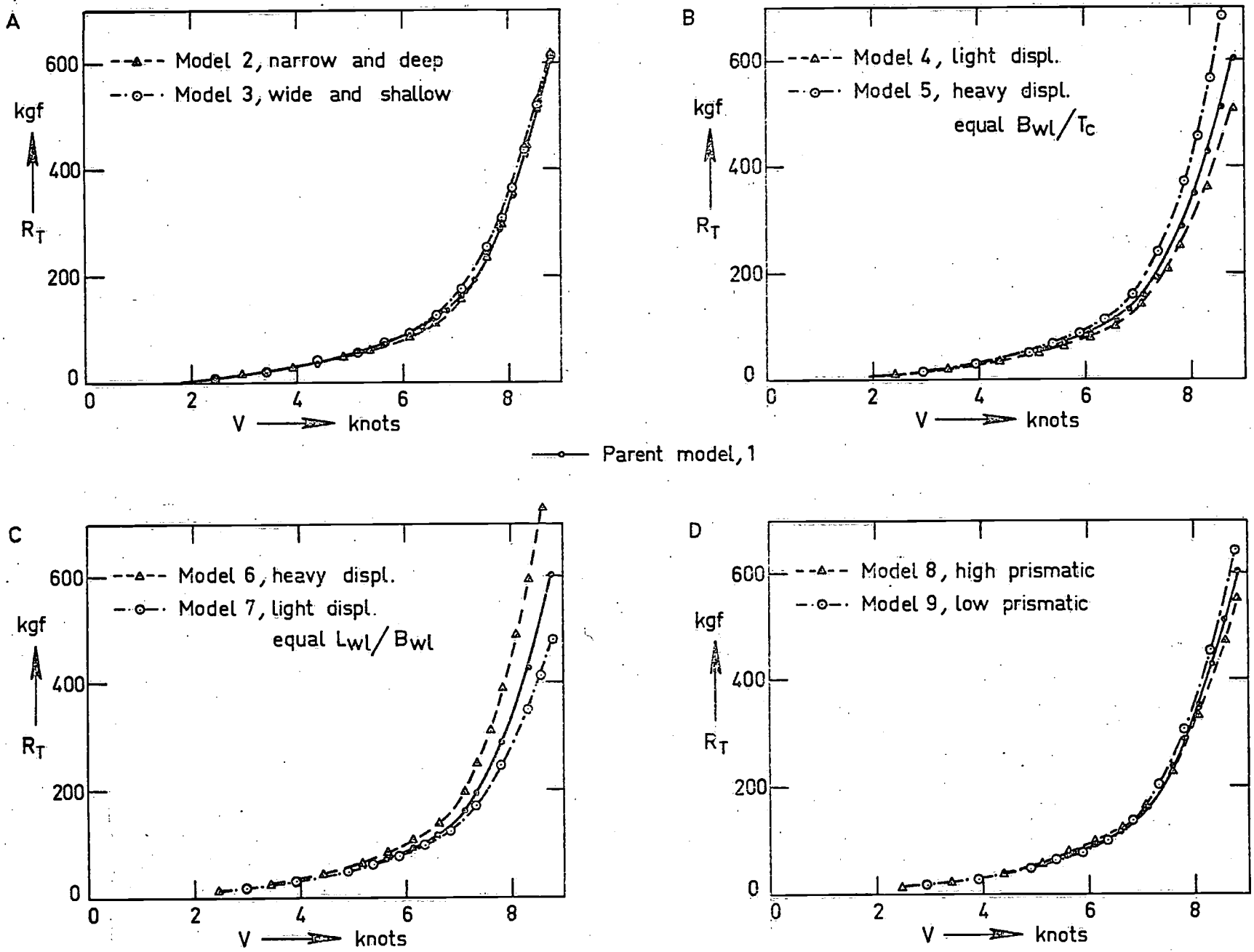

Fig.8 : Comparison of upright resistance. (L_{wl} = 10m)

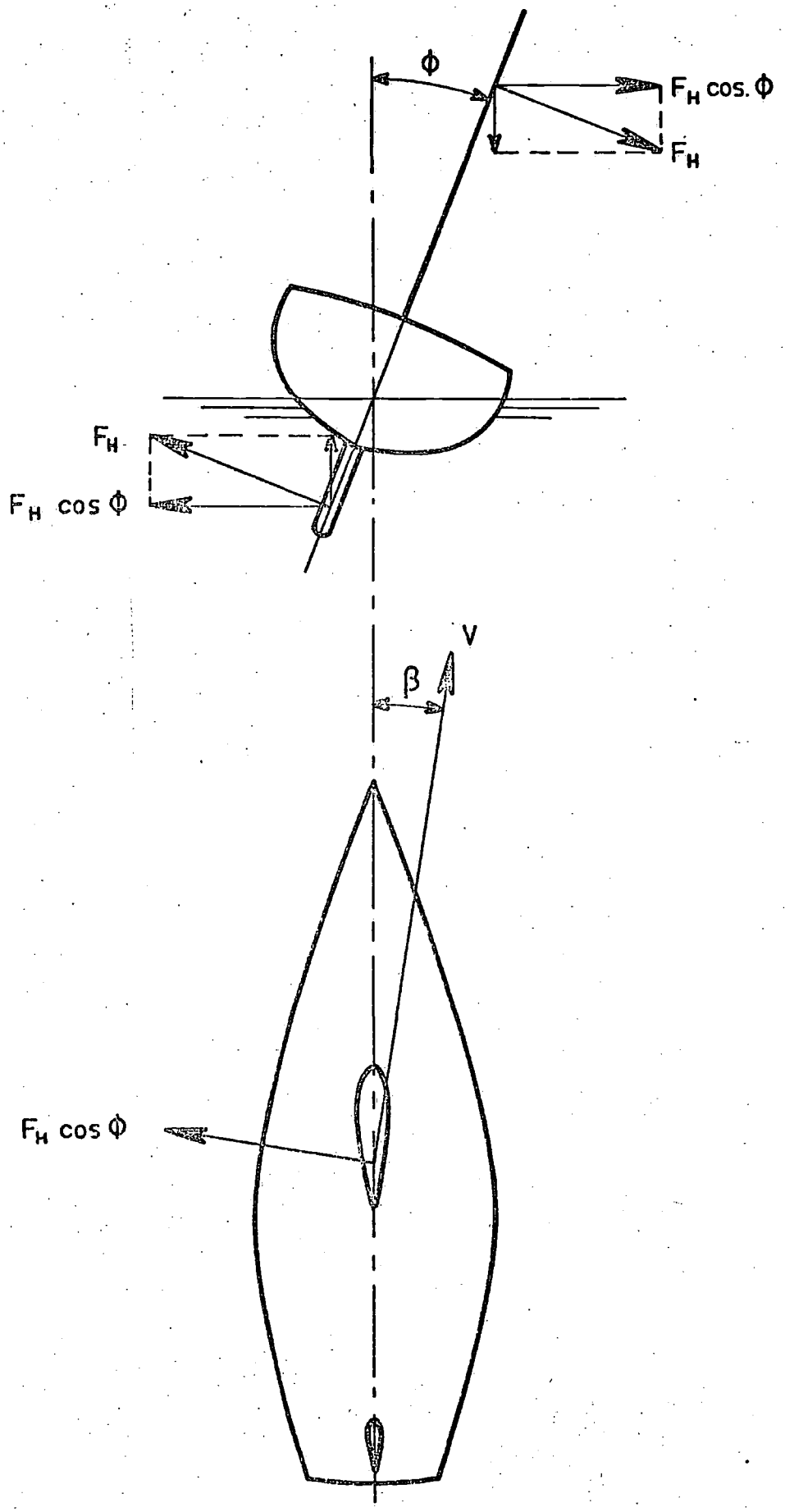

Fig. 9 : Sideforce and sailforce.

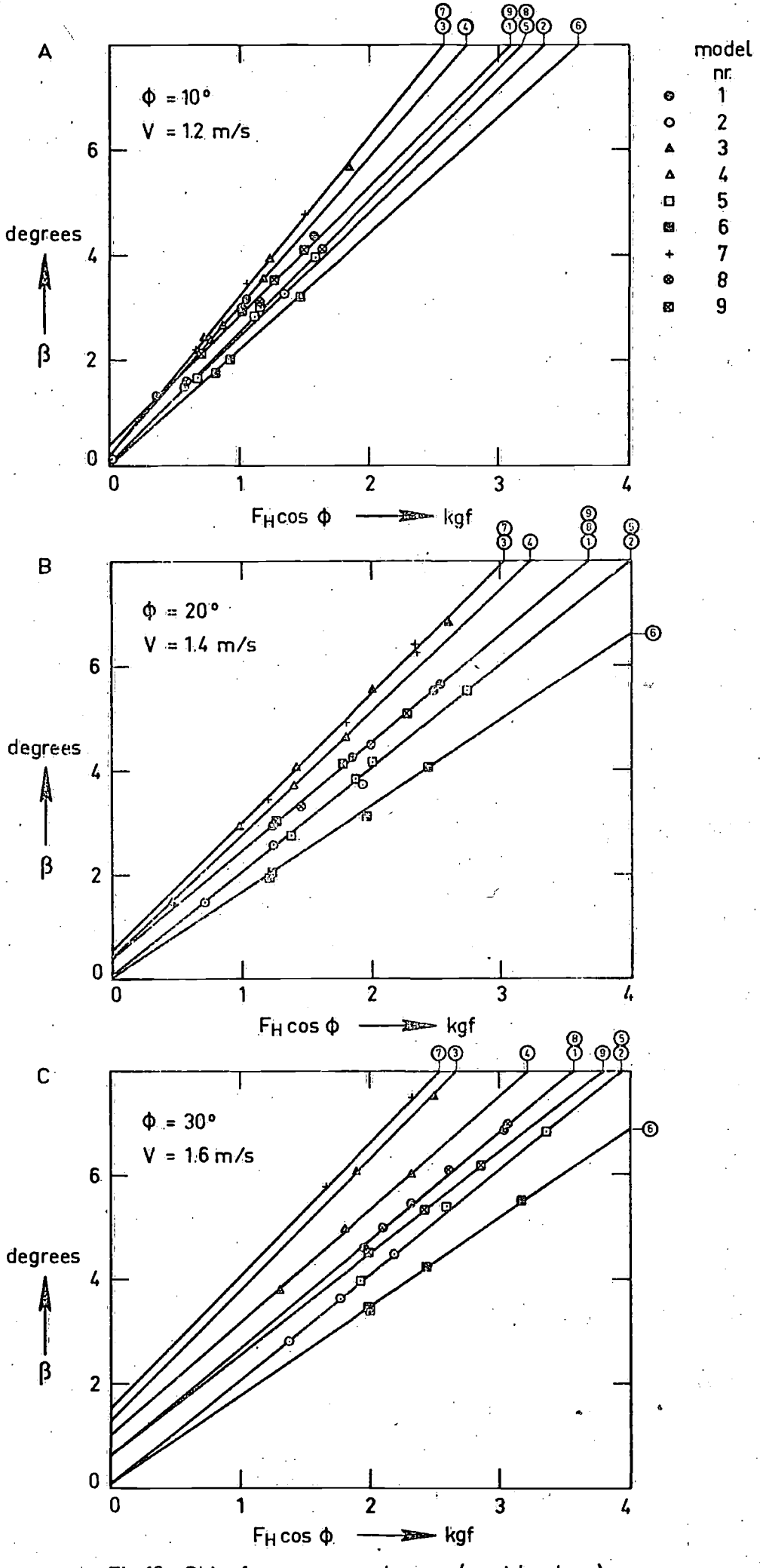

Fig. 10: Side force versus leeway (model values).

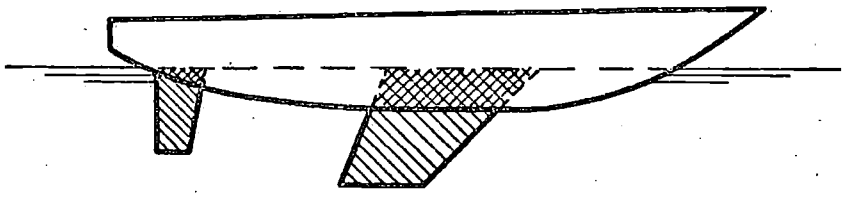

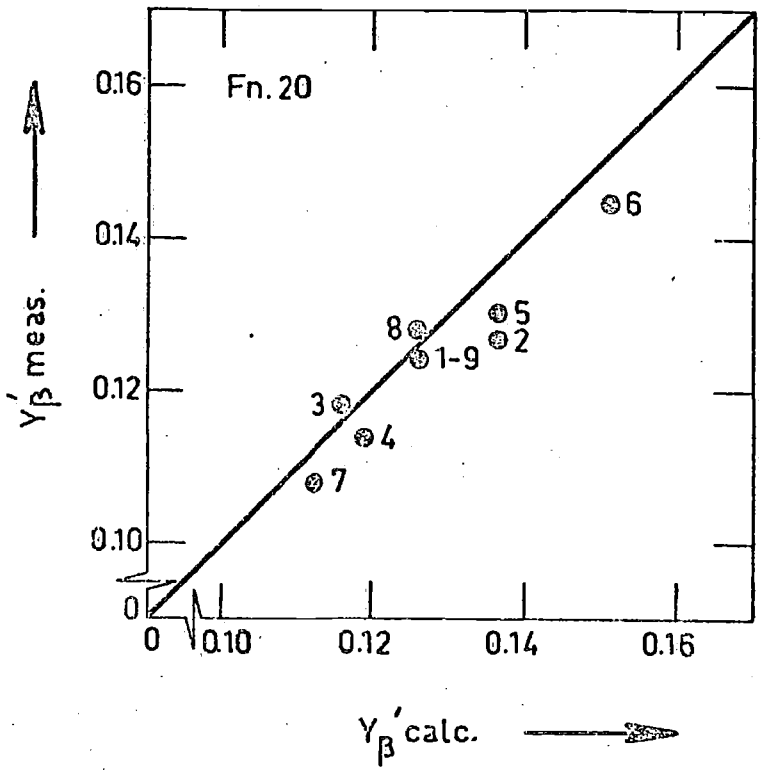

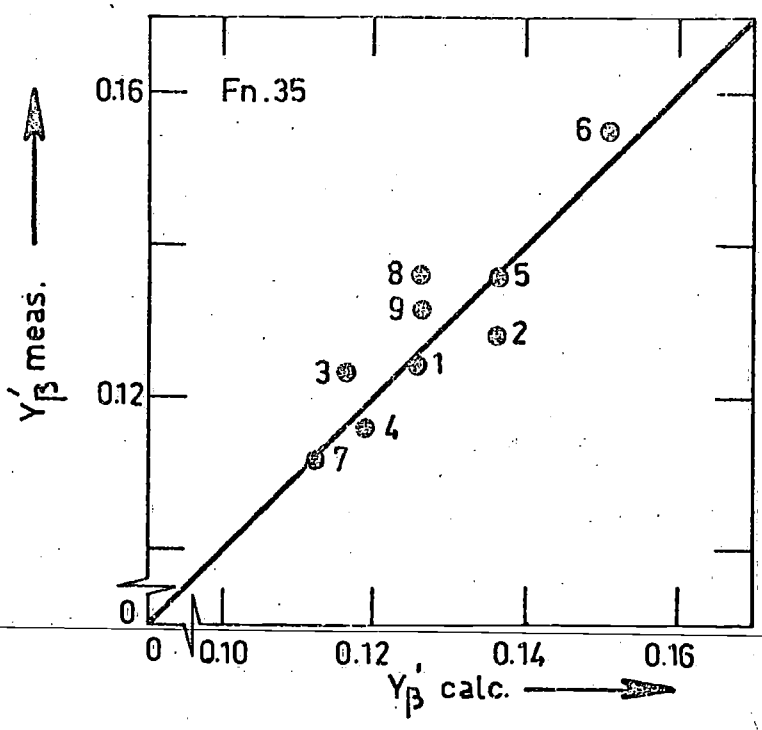

Fig.11: Calculated and measured side force curve slopes.

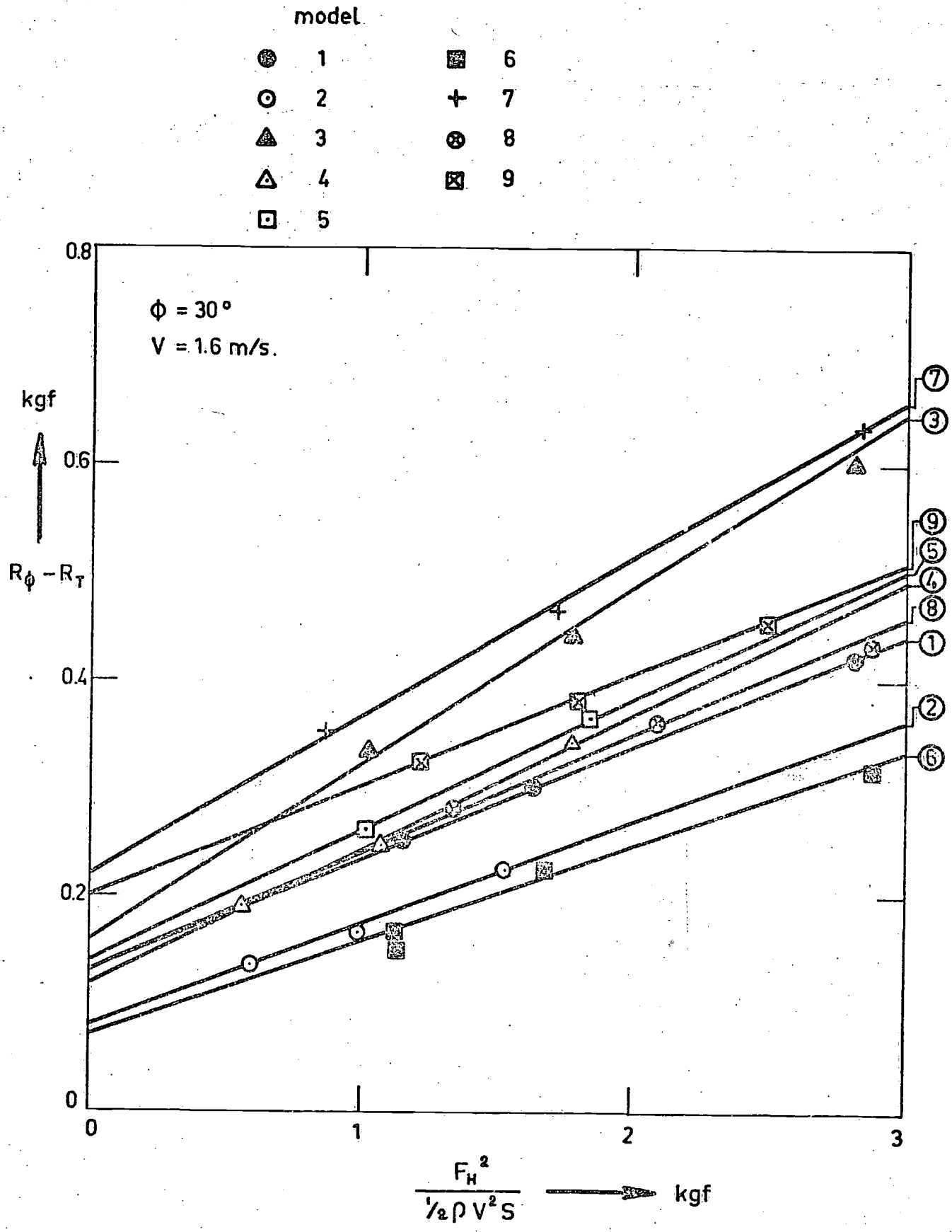

Fig. 12 : Heeled and induced resistance.

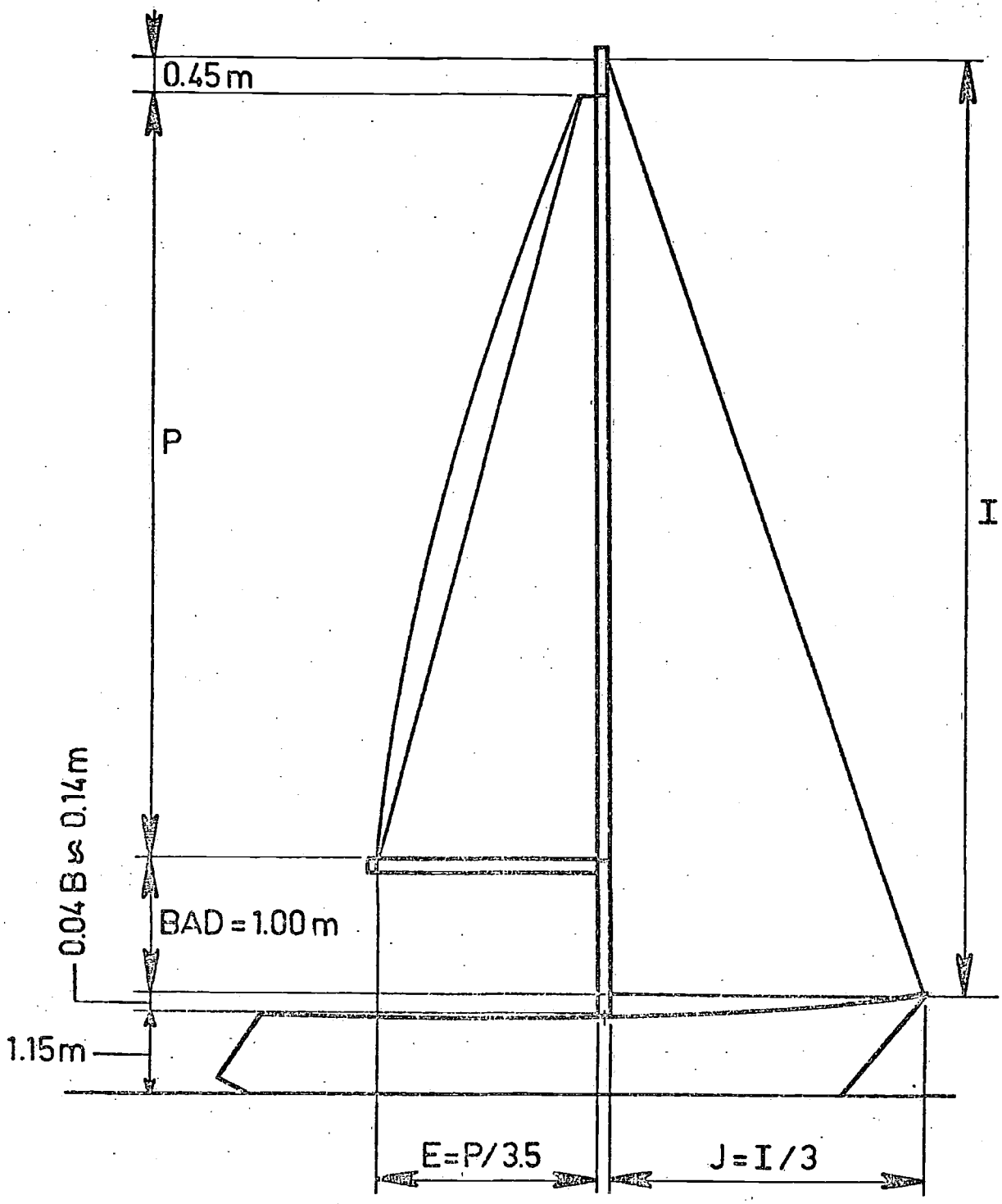

Fig. 13 : Standard sail plan design.

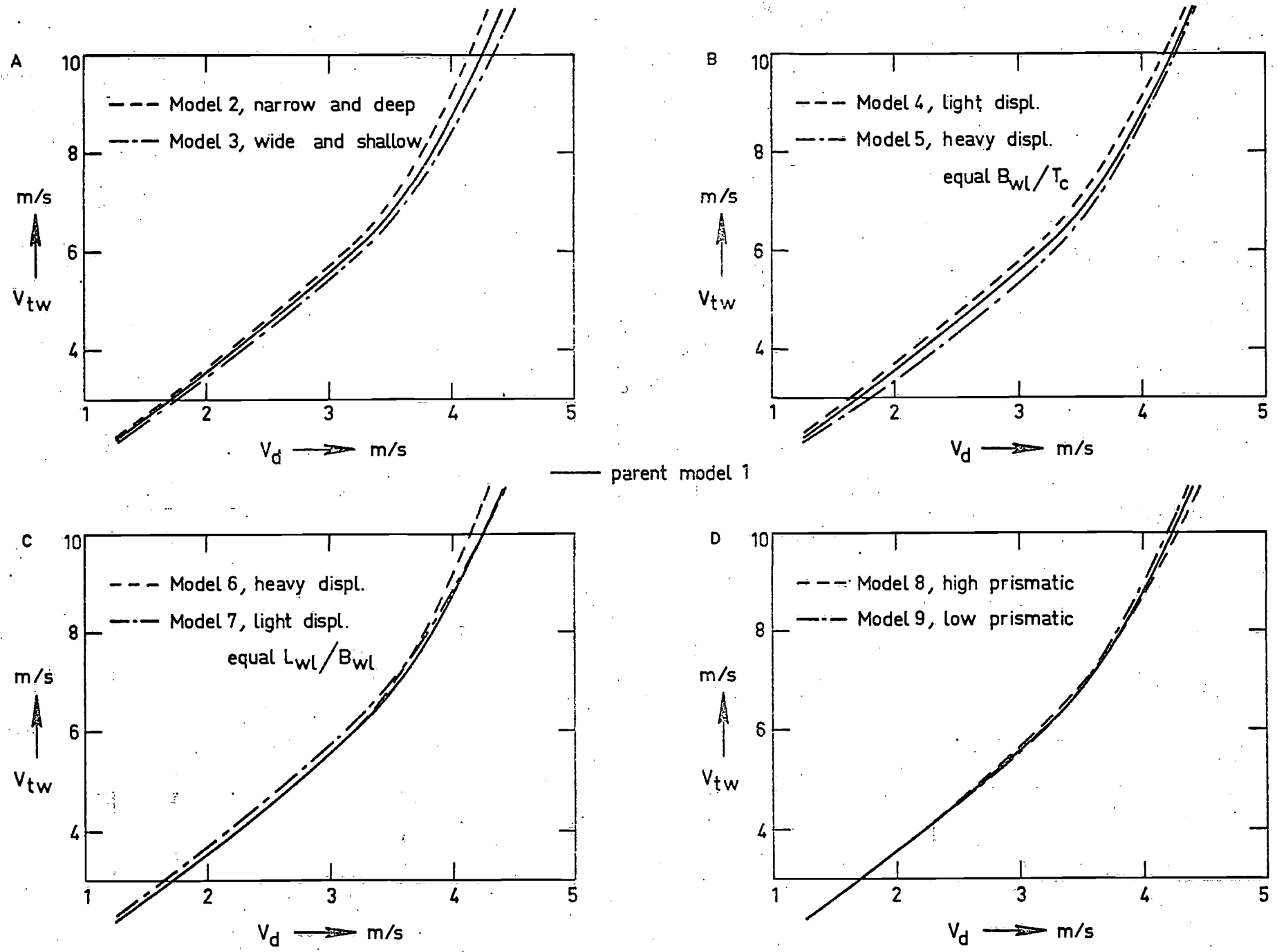

Fig. 14: Downwind speed.

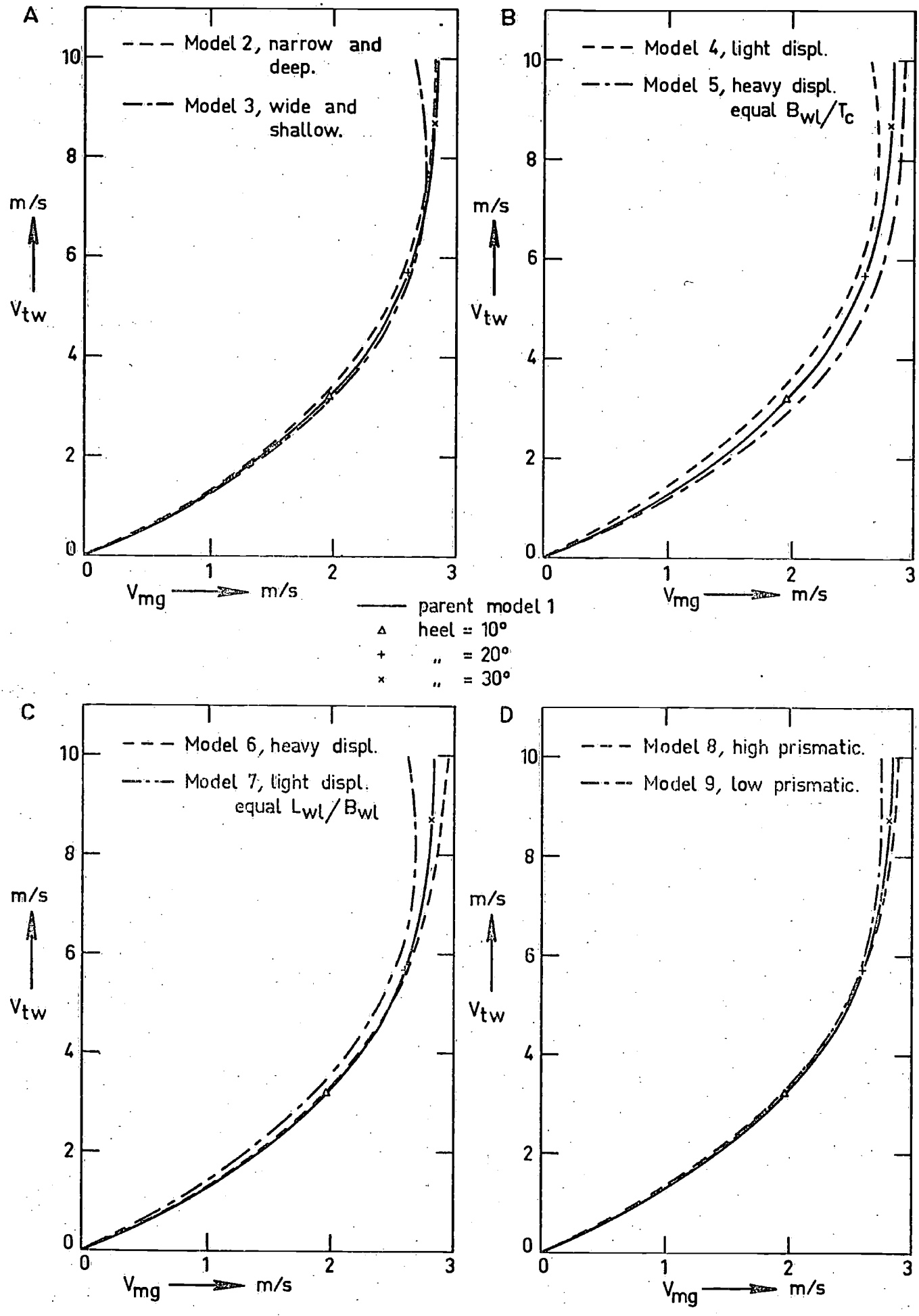

Fig. 15 : Speed – made – good to windward.

International **Shipbuilding** *Progress*

SHIPBUILDING AND MARINE ENGINEERING MONTHLY

devoted to theoretical and practical shipbuilding, marine-engine building and allied subjects; viz.

* ship hydrodynamics
* advanced techniques in shipping and ship design
* strength and hull vibration
* offshore and mooring problems
* ship manoeuvrability and control
* unconventinal ship types
* marine engineering
* small craft and dredgers
* cargo handling

Published by **INTERNATIONAL PERIODICAL PRESS**
193 Heemraadssingel, Rotterdam, the Netherlands
Telephone (010) 773325 Rotterdam
Telegrams INPRESS - Rotterdam
Bankers RABO-Bank, Rotterdam
Annual subscription rate Dfl. 105.00
(single copy Dfl. 9.50)

Volume 25 - July 1978 - No. 287

CONTENTS

Contributions for publication: Editors INTERNATIONAL SHIPBUILDING PROGRESS, Postbox 199, Delft, the Netherlands.

TEST RESULTS OF A SYSTEMATIC YACHT HULL SERIES

by

J. Gerritsma, G. Moeyes and R. Onnink*)

1. Introduction

Systematic research on the hydrodynamic characteristics of yacht hull forms has only been carried out on a rather limited scale. Already during the discussion of Davidson's classical paper on experimental studies of the sailing yacht, in 1936 [1], two of the discussers focussed the attention to the necessity of a systematic investigation of yacht hull forms, to give a more rational base for design methods and performance analysis. In this respect a parallel was drawn with the well-known Taylor Series, the results of which are still in use with naval architects to determine the resistance of merchant- and naval ships in the design stage [2]. This discussion took place some forty years ago, but already at that time those concerned with yacht research and yacht design were well aware of the fact that systematic design for sailing yachts could be extremely useful to analyse the influence of hull form and sailplan variations. The possibility to determine the performance of a yacht by varying the sail geometry and the stability of a given design. based on the results of one particular model test had been available for some time, and it was also possible to include in the analysis a variation of the yacht's size, keeping the same geometrical form. An additional possibility, to include form variations could be considered as a useful and even necessary extension of the existing methods. In this respect the rating of racing yachts is a special area of interest. The determination of a yacht's rating as a function of hull geometry, sail dimensions and stability is important because designers of racing yachts try to optimize hull and sails to produce an optimum combination of rating and speed potential. Rule makers aim at equal performance at equal rated length for fair competition.

There is no doubt that designers of cruising and racing yachts would benefit from the results of systematic model tests, although the problems are of such a complexity, that the full scale experiment, a "one off" will continue to play an important role in development of yacht desings.

Systematic model tests have been carried out for 12-meter yachts, because in this case the research costs for one individual design is not a very restrictive factor. Unfortunately most of the results of such tests are confidential and concern a rather extreme class of yachts.

An interesting systematic model series of yacht hulls has been presented by De Saix on the 2nd HISWA Symposium in 1971 [3]. He varied the lines of the parent model, Olin Stephens' "NY 32", to study the effect of the beam-draft ratio (5 models) and the prismatic coefficient (3 models). De Saix remarks in his paper:

> "It is hoped the work will encourage others in the same position as the author to contribute systematic data for the use of the individual yacht designer".

Gerritsma and Moeyes published the results of a small systematic series consisting of three models with equal waterline length, breadth and rating, but with a considerable variation in the length-displacement ratio [4]. With regard to fin keels and rudders, isolated or in connection with the hull, a reasonable amount of systematic work has been carried out by De Saix [5], Millward [6], Herreshoff and Kerwin [7], Beukelman and Keuning [8], and others. This summary is not considered as complete, but it may serve to give an impression of the hydrodynamic research on sailing yachts, other than model testing of individual designs.

The entire problem of yacht performance is very complex and includes also the sail forces. The combined knowledge of hull forces and sail forces can be used to simulate sailing conditions, for instance to determine the speed made good and the heel angle under given wind conditions. Computer techniques allow the analysis of a large amount of data and consequently many combinations of hull forms and sailplans can be considered when the basic hydrodynamic and aerodynamic data are available. To this end sail forces have to be known as a function of wind speed and apparent wind angle for the considered sail configuration. For the close-hauled condition the well known Gimcrack coefficients are commonly used. Some forty years ago these coefficients have been derived by Davidson from full scale tests with the yacht "Gimcrack" and corresponding yacht model tests [1]. The assumption being made was that in the equilibrium condition, defined by forward speed, heel angle and leeway angle, the driving sailforce is equal in magnitude but opposite in sign with the longitudinal water resistance force. The same holds for the heeling sailforce and the sideforce, acting on the under water part of the yacht. The hydrodynamic forces can be determined from experiments with a model running in the same conditions

*) Delft University of Technology, Ship Hydromechanics Laboratory, The Netherlands.

(speed, heel angle, leeway angle) as during full scale tests and consequently the sail forces follow from the above mentioned equalization of sail- and hull forces. It is assumed that the sail force coefficients, derived in this way are independent of the planform of the sails. Although the Gimcrack coefficients are restricted to the close-hauled condition, the method can be extended to other points of sailing. A theoretical calculation of sail forces with sufficient accuracy is not yet available, although attempts have been made by Milgram [15] to investigate the influence of planform on sail forces with vortex sheet calculations. In some special cases wind tunnel measurements with model sails have been carried out [9], [10]. Systematic model experiments with a sail configuration of a cruising sloop, for all points of sailing have been carried out by Wagner and Boese [11]. These wind tunnel tests included the main sail, the working jib, genoa and spinnaker, in combination with the part of the hull above the waterline, as well as the aerodynamic forces on the hull only. The various sail combinations were also tested without the hull. In view of the age of the Grimcrack measurements two new determinations of sail force coefficients have been carried out in 1974, using Davidson's method to combine model tests and full scale data. They concern the American yacht "Bay Bea" [12] and the Dutch yacht "Standfast" [13]. In the latter case the extensive model test program included the applied rudder angle, which could therefore be added to define the sailing condition to match the model and full scale results. The new data cover all points of sailing. The sail force coefficients derived with these experiments are larger than the "Grimcrack" values, which may be due to the more efficient sail plans and the modern materials, used for sail cloth.

The experience of testing a fair number of individual yacht designs in the Delft Ship Hydromechanics Laboratory led to the conclusion that, within the time available for yacht research, much more knowledge could be obtained by testing a systematic series of yacht hulls, with variations in hull form. This series was planned to contain primarily variations of length displacement ratio, prismatic coefficient and longitudinal position of the centre of buoyancy, and should consist of approximately 27 models to cover most types of yachts. In an early stage of planning a cooperation of Delft with the Department of Ocean Engineering of the Massachusetts Institute of Technology, Boston has been established in view of their H. Irving Pratt Ocean Race Handicapping Project. This cooperation comprises generating the lines and manufacturing polyester hulls and keels of the first 9 models by MIT; towing tank testing has been carried out by the Delft Ship Hydromechanics Laboratory. Unfortunately the funds of the Pratt-project do not permit MIT to cooperate in the testing of further models. The test results will be used by MIT to look for fair handicap systems, while after terminating the whole series the analysis of Delft intends to provide above all the designer with basic hydrodynamic design knowledge and performance estimation methods. In this paper the resulsts of the first nine models are discussed. A standard performance calculation has been carried out for each of the nine models, assuming a waterline length of 10 meters, a realistic sail plan and a stability conforming the present design practice for I.O.R. designs. This exercise enables the comparison of the performance of the nine models with the rating according to the I.O.R.

2. Geometric description of the systematic series

The main form parameters of the first nine models are given in Table 1, in which model 1 represents the parent form. All models have approximately the same longitudinal location of the centre of buoyancy. The prismatic coefficient has an nearly equal value for models 1 - 7, whereas model 8 has a high and model 9 a low prismatic coefficient. The relations between the various main parameters are presented in Figure 1 for models 1 - 9 (black spots) as well as for thirteen models to be investigated in the near future (open circles). The lines of the nine models are shown in Figure 2. Wider, narrower, deeper and shallower models have been derived from the parent model by multiplication of coordinates with a factor which is constant for the underwater part and gradually going to 1 for the above water part of the hull. The resulting cross-sections, waterlines and buttocks were faired by computer graphics with spline cubic equations, while slight corrections of the profile ends fore and aft were introduced, when necessary, to obtain more regular and realistic forms. These corrections cause the minor differences in LCB and prismatic as shown in

Table 1
Main form parameters

model nr.	L_{WL}/B_{WL}	B_{WL}/T_c	C_p	$L_{WL}/V_c^{1/3}$	LCB_c %
1	3.17	3.99	0.568	4.78	−2.29
2	3.64	3.04	0.569	4.78	−2.29
3	2.76	5.35	0.565	4.78	−2.31
4	3.53	3.95	0.564	5.10	−2.32
5	2.76	3.96	0.574	4.36	−2.44
6	3.15	2.98	0.568	4.34	−2.38
7	3.17	4.95	0.562	5.14	−2.31
8	3.32	3.84	0.585	4.78	−2.37
9	3.07	4.13	0.546	4.78	−2.19

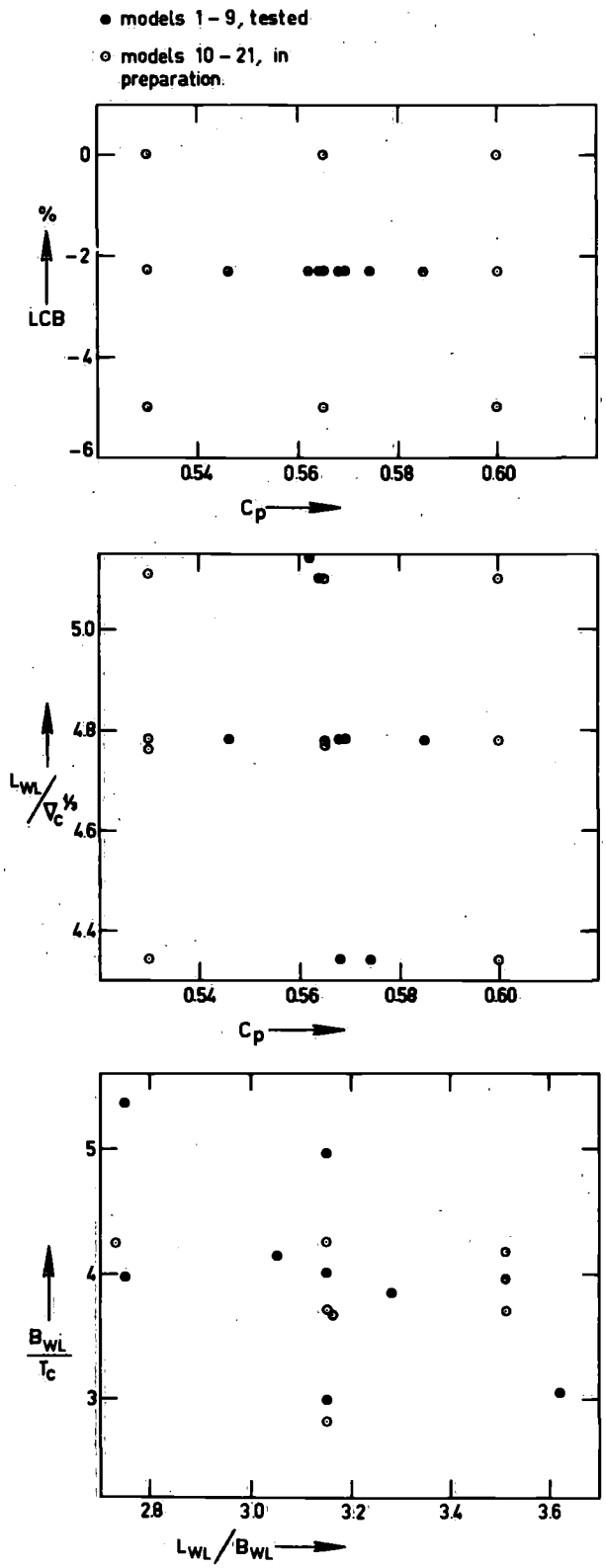

Figure 1. Form parameters of model series.

Table 1. Variation of the prismatic coefficient was accomplished by shifting cross-sections to obtain the desired curve of cross sectional areas belonging to the prescribed C_p and LCB.

The parent model, which resembles closely the succesful "Standfast 43" designed in 1970 by Frans Maas of Breskens, has a moderate form with regard to ratio's of main dimensions. It has clean lines, without bustles or other extreme variations in the curvature of the hull surface. With regard to the parent model, model 2 is narrow and deep, whereas model 3 is wide and shallow, where draught is referred to the canoe body. They have the same displacement as the parent. Models 4 and 5 have a constant beam-draught ratio, but nr. 4 is lighter and nr. 5 is heavier than the parent hull. Models 6 and 7 are variations in displacement at constant length-beam ratio, thus having variations in the beam-draft ratio. Model 6 is heavier and deeper, whereas model 7 is lighter and shallower. Model 8, with the high prismatic has fuller ends and Model 9 with the low prismatic coefficient has fine end sections.

Because hull form variations were the main object of the series, all models have been tested with the same fin keel and rudder. Consequently deep- and shallow hull forms have an equal keel span, although this is not common design practice. A NACA 632-015 airfoil section has been used for the fin keel and a NACA 0012 section for the rudder. The arrangement of keel and rudder is shown in Figure 3.

The waterline length of the corresponding full scale "Standfast 43" is 10 meters, so far a first analysis of the experiments the scale factor of all models has been set to $\alpha = 6.25$ and test results have been extrapolated to 10 m waterline yachts. The main dimensions of these nine yachts and some other hull data are summarized in Tables 2A and 2B. Some of the derived quantities, such as wetted surface, metacentric radius etc. are given for the canoe body as well as for the combination canoe body plus keel plus rudder. The series of nine models is to small to derive empirical relations between the main dimensions and for instance the metacentric radius $\overline{BM}$ or the height of the centre of buoyancy above the keel $\overline{KB}$. It has to be noted that the keelpoint K is assumed to lie on the base line, which is the horizontal tangent to the canoe body. From Table 2B it may be concluded that the influence of the keel and rudder volume on the vertical position of the metacenter M is quite large. This influence should not be neglected in a calculation of the initial stability of a yacht. The computed static stability for heel angles up to 90 degrees is given in dimensionless form in Figure 4, where the residuary stability k (ϕ) is plotted on a base of heel angle ϕ for each of the nine models. The definition of the dimensionless residuary stability is given by:

$$k(\phi) = \frac{\overline{MN} \sin \phi}{\overline{BM}} \qquad (1)$$

and the meaning of $\overline{MN}$ in this expression is clarified

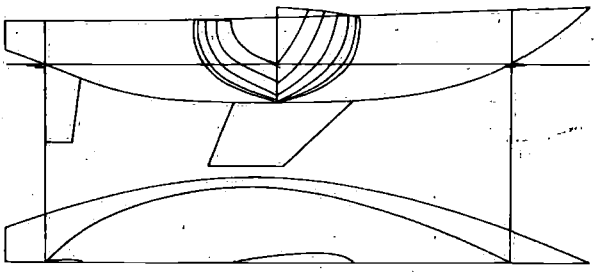

PARENT MODEL NR.1

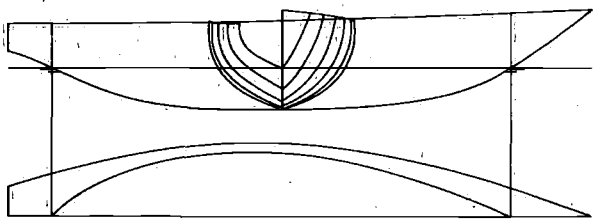

NR.2

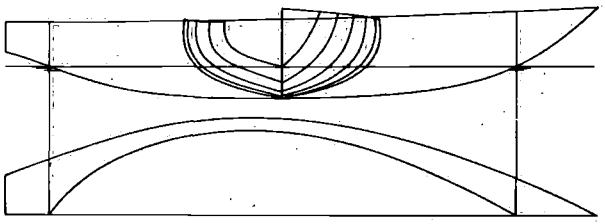

NR.3

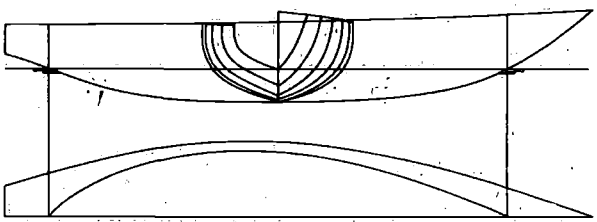

NR.4

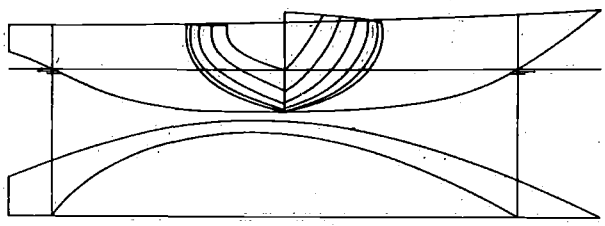

NR.5

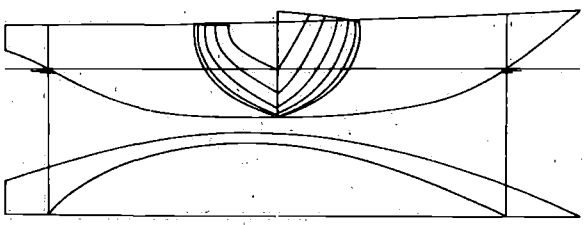

NR.6

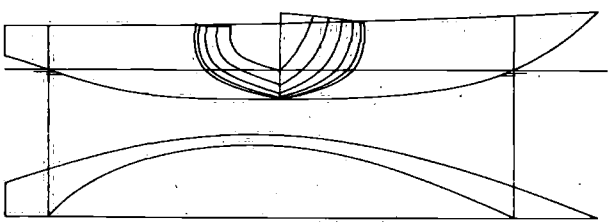

NR.7

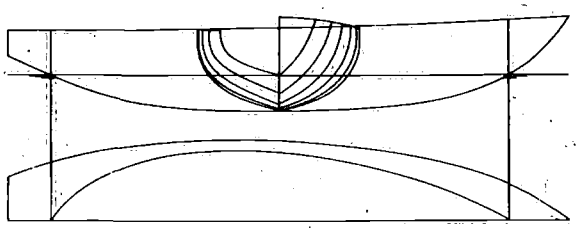

NR.8

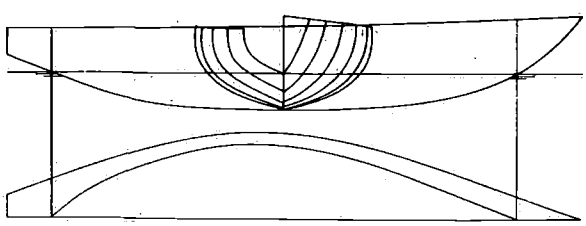

NR.9

Figure 2. Lines of models 1 - 9.

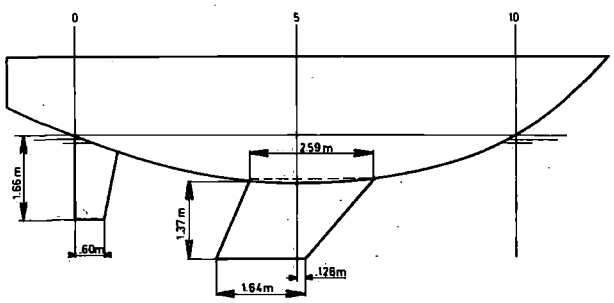

Figure 3. Fin keel and rudder arrangement.

in Figure 4. For geometric similar hull forms, which could have different dimensions, the arm of the static stability moment at a heel angle ϕ follows from:

$$\overline{GN} \sin\phi = \overline{GM} \sin\phi + k(\phi)\, \overline{BM} \qquad (2)$$

where $\overline{GM}$ and $\overline{BM}$ correspond to the considered dimensions of the yacht. The relative importance of the residuary stability $\overline{MN}$ sin ϕ is shown in Figures 5a and 5b, where the stability curves of models 2 and 3 (narrow and wide) are compared, assuming realistic values for the height of the centre of gravity G. For model 2 the influence of the residuary resistance is not important, whereas for model 3 $\overline{MN}$ sin ϕ is relatively large. It is concluded that for detailed studies of a yacht's stability the determination of the initial stability ($\overline{GM}$ sin ϕ) is not sufficient. In particular for wide beam hulls the residuary stability is rather important. The effect of the yacht's own wave system is not considered in this static stability calculations.

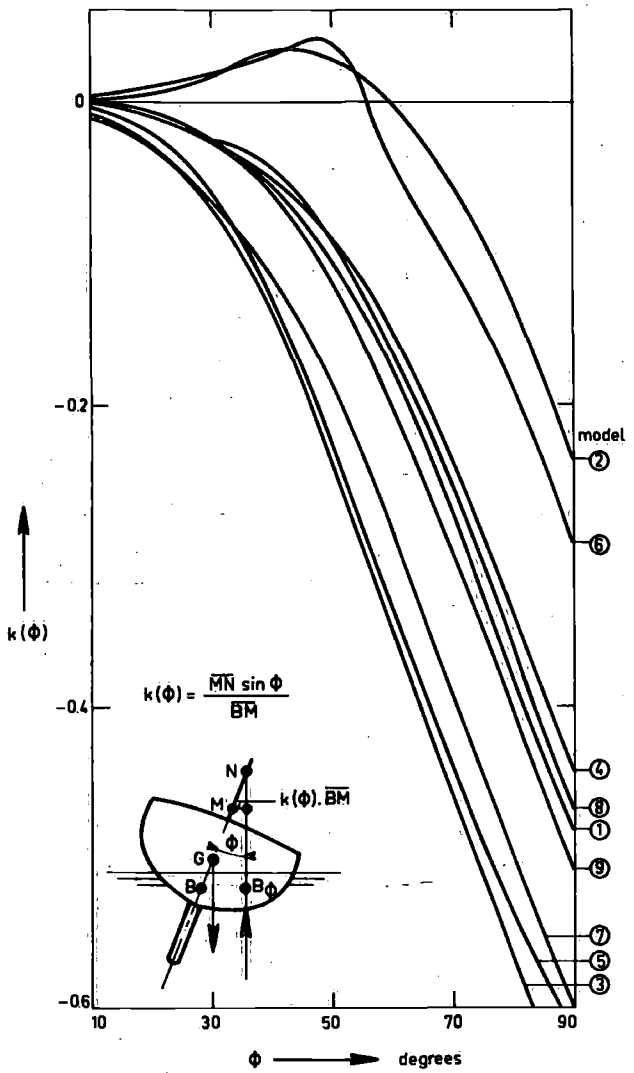

Figure 4. Non-dimensional residuary stability, models 1 - 9, canoe body only.

3. Experimental set-up and test results

3.1 Experimental set-up

All models were constructed of GRP, corresponding to a linear scale ratio 6.25 and a waterline length of 1.6 m. This size, which implies an overall length of about 7 feet, fits the usual measuring apparatus of the Delft Ship Hydromechanics Laboratory and gives in combination with the applied turbulence stimulator an adequate guarantee for consistent test results. This turbulence stimulator consists of carburundum strips on hull, keel and rudder, which arrangement is shown in Figure 6. The carburundum has a grainsize 20 and is applied on the models with a density of approximately 10 grains/cm^2. Upright resistance tests for

Table 2a
Main dimensions and derived quantities

Nr	L_{OA} m	L_{WL} m	B_{MAX} m	B_{WL} m	T_C m	D m	F m	V_C m^3	S_C m^2	A_X m^2	A_W m^2
1	12.65	10.04	3.67	3.17	0.79	1.94	1.15	9.18	25.4	1.62	21.8
2	12.65	10.04	3.21	2.76	0.91	2.06	1.15	9.18	23.9	1.62	19.1
3	12.65	10.06	4.25	3.64	0.68	1.83	1.15	9.16	27.6	1.63	25.2
4	12.65	10.06	3.32	2.85	0.72	1.87	1.15	7.55	23.0	1.34	19.8
5	12.65	10.05	4.24	3.64	0.92	2.07	1.15	12.10	29.1	2.15	25.3
6	12.65	10.00	3.66	3.17	1.06	2.21	1.15	12.24	27.5	2.16	21.9
7	12.65	10.06	3.68	3.17	0.64	1.79	1.15	7.35	24.1	1.31	21.8
8	12.65	10.15	3.54	3.05	0.79	1.94	1.15	9.18	25.4	1.57	22.1
9	12.65	10.07	3.81	3.28	0.79	1.94	1.15	9.18	25.0	1.68	21.5

	volume m^3	wetted area m^2
keel	0.639	6.01
rudder	0.055	2.15
total	0.694	8.16

Table 2b
Main dimensions and derived quantities

Nr	I_T m^4	I_L m^4	LCF %	LCB %	$\overline{KB}^*$ m	$\overline{BM}^*$ m	$\overline{KM}^*$ m	$\overline{KB}^{**}$ m	$\overline{BM}^{**}$ m	$\overline{KM}^{**}$ m
1	12.89	113.2	−3.32	−2.29	0.53	1.40	1.93	0.45	1.30	1.75
2	8.64	99.2	−3.31	−2.29	0.60	0.94	1.54	0.56	0.87	1.43
3	19.88	131.1	−3.30	−2.31	0.45	2.17	2.62	0.38	2.02	2.40
4	9.60	102.8	−3.30	−2.32	0.48	1.27	1.75	0.39	1.16	1.55
5	19.99	131.2	−3.32	−2.44	0.61	1.60	2.21	0.55	1.51	2.06
6	12.85	113.2	−3.34	−2.38	0.71	1.05	1.76	0.64	0.99	1.63
7	12.85	109.8	−3.29	−2.31	0.43	1.75	2.18	0.34	1.60	1.94
8	12.66	120.6	−3.43	−2.37	0.53	1.38	1.91	0.45	1.28	1.73
9	13.21	105.3	−3.07	−2.19	0.52	1.43	1.95	0.45	1.33	1.78

* canoe body
** canoe body + keel + rudder

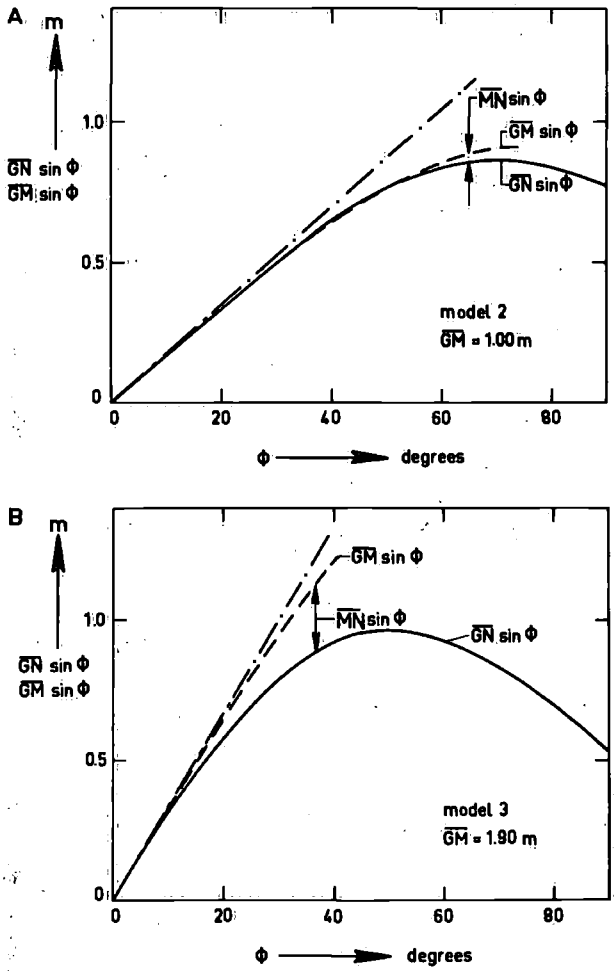

Figure 5. Stability curves models 2 and 3.

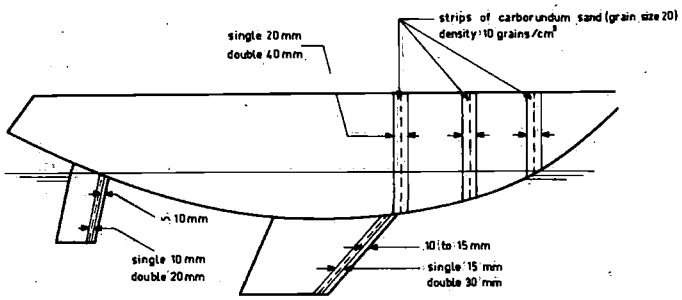

Figure 6. Turbulence stimulator.

model speeds of 0.5 m/s - 1.8 m/s (F_n 0.13 – 0.46) are carried out twice, with a "single" and a "double" sand strip to enable the extrapolation of the measured resistance values to zero sand strip width. It is then assumed that the extra resistance due to the sand strips varies with the speed squared and the strip width. Mean values of the resistance coefficients of the strips were determined in the middle of the tested speed range (V = 1.0 - 1.6 m/s) to avoid influence of special flow phenomena (laminar flow or wave-making). All tests have been carried out in tank nr. 2 of the Delft Ship Hydromechanics Laboratory, which has a wetted cross section of 1.22 x 2.75 m. In view of tank blockage effects the models 1, 6 and 7 have also been tested in tank nr. 1 (wetted cross section 2.55 x 4.22 m). All resistance values, as measured in the small tank wei corrected for blockage using the method given in [14] after checking the corrections with the tank nr. 1 results.

In addition to the upright resistance tests, for each of the nine models heeled and leeway tests are carried out. Heel angles of 10, 20 and 30 degrees and leeway angles up to 10 degrees have been considered. Model speeds are chosen as 1.0, 1.2 and 1.4 m/s at 10 degrees, 1.2, 1.4 and 1.6 m/s at 20 and 30 degrees heel. With these combinations of variables all practical sailing conditions may be covered. During the tests heel angles are the result of the side force due to leeway and forward speed and to a moment produced by a weight p to be shifted transversely over a distance t. This additional heeling moment is necessary first of all because the model is fixed sideways to measure the side force, and the locations where the reaction forces are measured do not correspond with the centre of

effort of sail forces. Secondly the model centre of gravity is not scaled down exactly from full scale size, which necessitates a correction for stability. The additionally applied moment is varied in magnitude to allow for an analysis with various positions of the centre of sail forces (sail plan) and centre of gravity (stability).

3.2. Upright resistance

For each of the nine models the residuary resistance per ton displacement of the canoe body R_R/Δ_c is given in Table 3 as a function of Froude number $F_n = V/\sqrt{gL_{WL}}$. For this comparison only displacement of the canoe body is considered because the influence of keel and rudder on residuary (mainly wave making) resistance is considered to be of minor importance. For geometric similar hull form the residuary resistance is found from:

$$R_R = R_R/\Delta_c \times \Delta_c \quad \text{(kgf.)} \tag{3}$$

where: Δ_c is the displacement of the canoe body. The corresponding speed is:

$$V = F_n \times \sqrt{gL_{WL}} \tag{4}$$

where:

g = 9.81 m/s^2.

L_{WL} = nominal length of waterline in m.

To find the total resistance R_T the frictional resistance R_F is added,

$$R_T = R_R + R_F \tag{5}$$

For yachts with separated fin keel and rudder the frictional resistance is found as the summed contributions of canoe body, keel and rudder:

$$R_F = \tfrac{1}{2}\rho V^2 (S_c C_{F_c} + S_k C_{F_k} + S_r C_{F_r}) \tag{6}$$

where:

S_c, S_k and S_r are wetted area of canoe body, keel and rudder respectively.

C_{F_c}, C_{F_k} and C_{F_r} is frictional resistance coefficient for respective parts.

ρ is density of water at 15° C

= 101.87 kgm^{-1}S^2 for fresh water

= 104.61 kgm^{-1}S^2 for salt water.

The frictional resistance coefficient is calculated according to the definition by the International Towing Tank Conference 1957

$$C_F = \frac{0.75}{(\log R_n - 2)^2} \tag{7}$$

where the Reynolds number is calculated for canoe body, keel and rudder as respectively:

$$R_{n_c} = \frac{V \times 0.7\, L_{WL}}{\nu}$$

$$R_{n_k} = \frac{V \times \bar{C}_k}{\nu} \tag{8}$$

$$R_{n_r} = \frac{V \times \bar{C}_r}{\nu}$$

Table 3

Residuary resistance per ton hull displacement

F_n \ nr	R_R/∇_c kg/ton								
	1	2	3	4	5	6	7	8	9
0.127	0.12	0.05	0.10	0.20	0.17	0.14	0.29	0.21	0.16
0.153	0.29	0.19	0.32	0.37	0.24	0.28	0.47	0.41	0.34
0.178	0.50	0.40	0.59	0.69	0.37	0.46	0.74	0.68	0.58
0.203	0.82	0.70	0.92	0.97	0.58	0.76	1.12	1.01	0.90
0.229	1.26	1.13	1.40	1.43	0.93	1.19	1.66	1.44	1.31
0.254	1.94	1.69	2.12	2.09	1.43	1.83	2.36	2.11	1.86
0.267	2.36	2.05	2.57	2.50	1.84	2.18	2.84	2.57	2.24
0.280	2.79	2.52	3.19	2.98	2.30	2.72	3.25	3.16	2.66
0.292	3.38	2.97	3.85	3.56	2.84	3.20	3.73	3.88	3.12
0.305	3.99	3.50	4.47	4.20	3.37	3.72	4.35	4.64	3.67
0.318	4.61	4.16	5.10	4.75	4.16	4.35	5.23	5.33	4.35
0.330	5.30	4.99	6.01	5.56	4.92	5.07	6.27	6.16	5.23
0.343	6.38	6.24	7.30	6.92	6.07	6.27	7.53	7.31	6.45
0.356	7.99	7.99	9.20	8.81	7.91	8.02	9.05	8.78	8.33
0.369	10.51	10.45	11.70	11.19	10.26	10.57	11.35	10.85	11.04
0.381	13.55	13.79	14.96	14.55	13.83	14.21	14.43	13.62	14.71
0.394	17.89	18.52	19.15	18.76	17.95	18.85	18.32	17.25	19.51
0.407	23.04	24.46	24.26	24.07	23.70	25.07	23.21	21.75	25.25
0.419	29.31	31.39	30.48	30.38	30.40	32.66	29.23	27.21	32.09
0.432	37.05	39.42	37.86	37.79	38.89	41.27	36.15	33.67	40.01
0.445	45.88	48.31	46.43	46.21	48.10	51.58	44.03	41.24	49.18
0.458	55.45	57.33	55.89	55.51	59.21	62.55	52.74	49.60	59.73

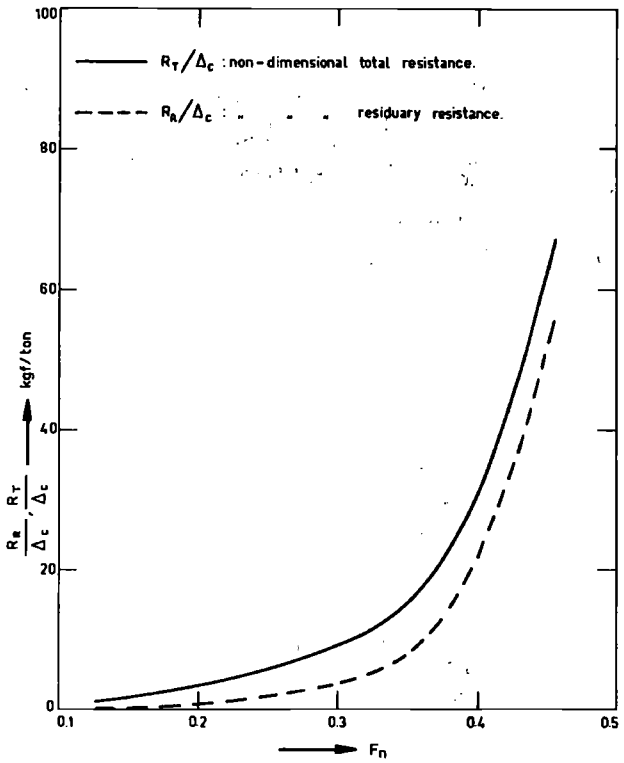

Figure 7. Non-dimensional resistance of model 4.

with:

$\nu = 1.1413 \times 10^6$ for fresh water of 15° C

$\nu = 1.1907 \times 10^6$ for salt water of 15° C

$\overline{C_k}$ and $\overline{C_r}$ are the average chord length of keel respectively rudder in m.

The factor 0.7 in the definition of the Reynolds number for the canoe body allows for the particular profile and waterline shape of a yacht and gives a kind of average wetted length. The date in Table 3 is obtained from measurements being corrected for the effects of sand strips and tank blockage.

As an example the total and residuary resistance of model 4 are given in dimensionless form in Figure 7 to show the relative importance of the resistance components. At a Froude number $F_n = 0.35$, which is approximately the maximum speed in the close-hauled condition the frictional and residuary resistance are about equal in magnitude.

To compare the upright resistance of the hull form variations Figures 8a, b, c and d give the total resistance in upright condition for a waterline length L_{WL} = 10 m. Four groups are considered:

Figure 8a compares the parent model with models 2

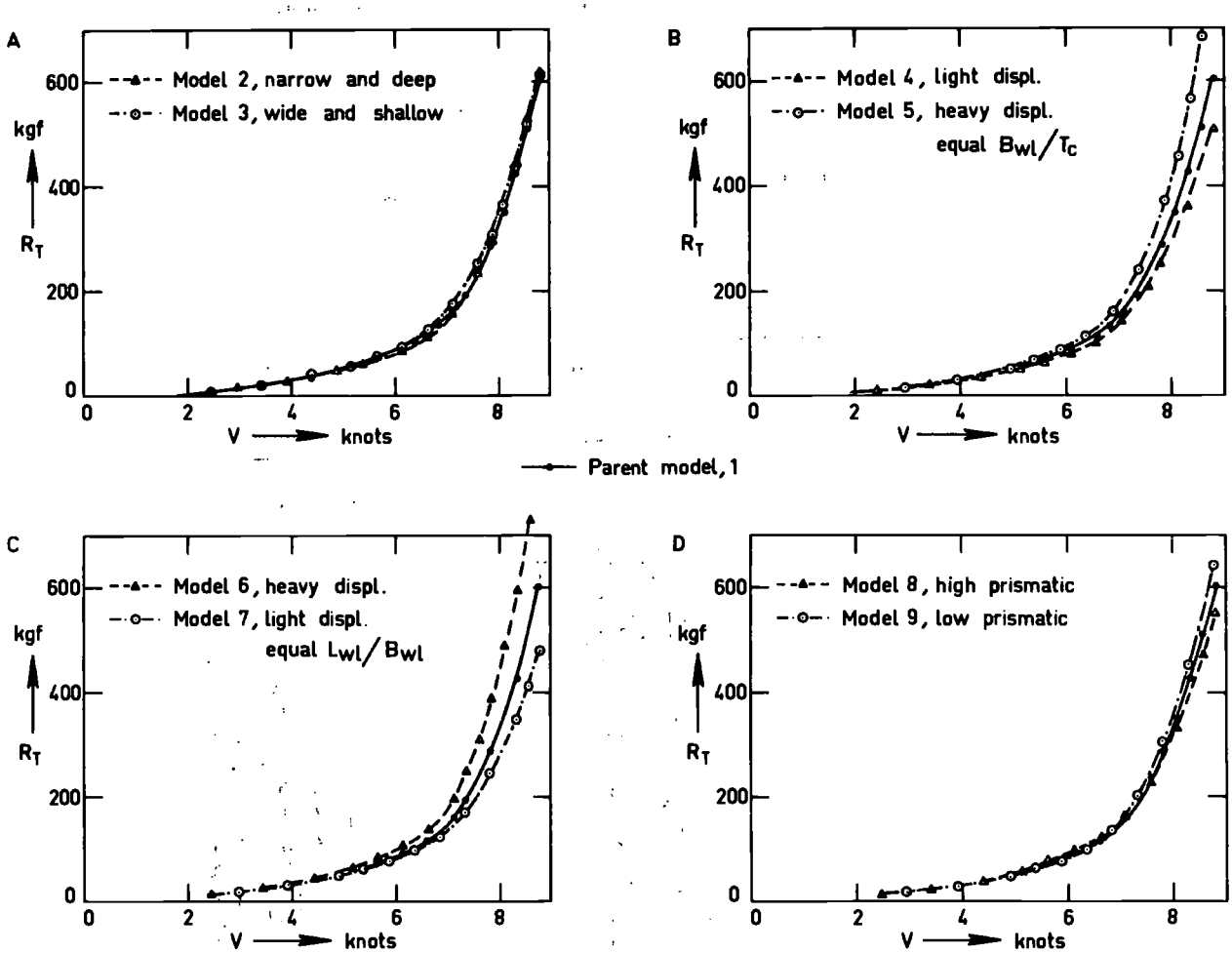

Figure 8. Comparison of upright resistance (L_{WL} = 10 m).

and 3 (equal displacement, narrow and deep versus wide and shallow).

Figure 8b compares models 1, 4 and 5 (equal B_{WL}/T_c, medium, light and heavy displacement).

Figure 8c compares models, 1, 6 and 7 (equal L_{WL}/B_{WL}, medium, heavy and light displacement).

Figure 8d compares models 1, 8 and 9 (medium, high and low prismatic).

The Figures show the primary importance of the length-displacement ratio with regard to resistance (models 4, 5, 6 and 7), the relatively small influence of the beam-draught ratio and the beneficial effect of a high prismatic coefficient at speeds above 6¾ knots for the considered length of waterline.

Table 3 and equations 3 – 8 enable the determination of the upright resistance of geometric similar yacht forms of given dimensions. Within the range of variation the data can be used for systematic studies of yacht hull resistance.

3.3. Side force and leeway

In any asymmetrical position the hull, keel and rudder develop a side force due to hydrodynamic action. The dominant parameter in this respect is the leeway angle β, but also the heel angle ϕ and the rudder angle are causing side forces, of which the horizontal component is denoted by $F_H \cos \phi$, (see Figure 9). Although the rudder angle is important in this respect [13] this parameter is not considered here, because the object of the systematic series is to study the influence of hull form variations only. In Figure 10 a plot has been made of model side force versus leeway angle for heel angles 10, 20 and 30 degrees and model speeds respectively 1.2 m/s, 1.4 m/s and 1.6 m/s (corresponding to Froude numbers, 0.30, 0.35 and 0.40). These speeds are somewhat higher than optimal sailing speeds

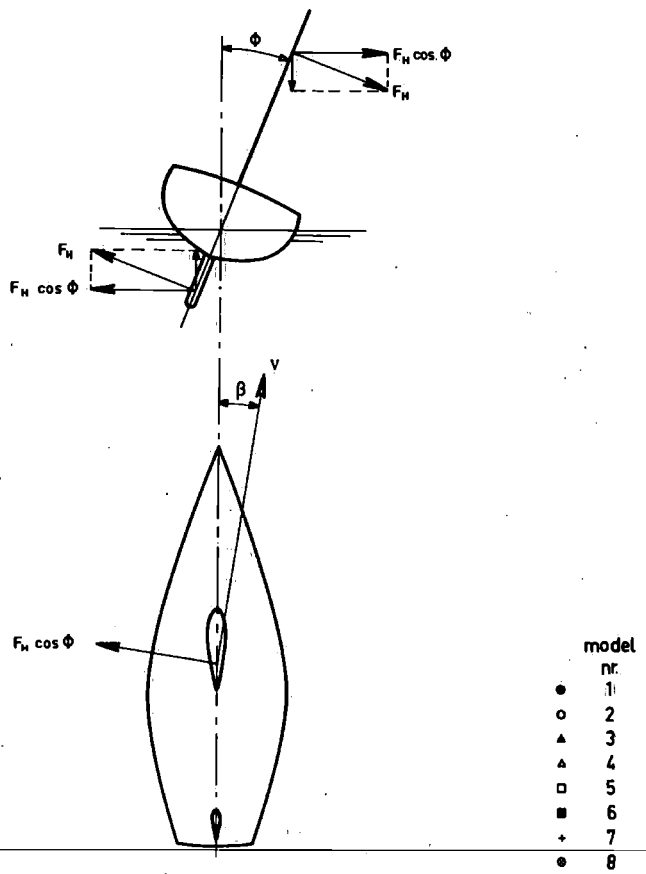

Figure 9. Side force and sail force.

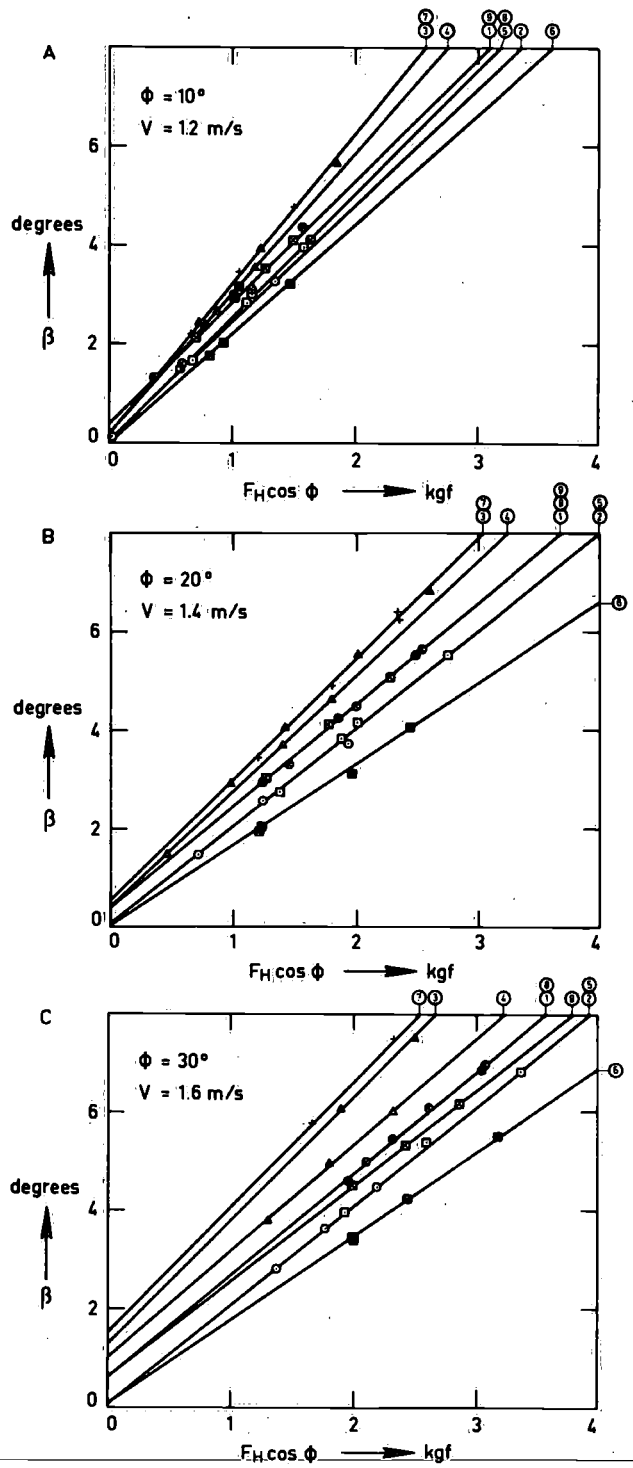

Figure 10. Side force versus leeway (model values).

in the close-hauled condition, but the figures may serve to illustrate some general conclusions regarding the ability to generate side forces for each of the nine models. However it should be remembered that all models had the same fin keel and rudder. Figure 10c shows that model 6 (heavy displacement, deep hull) needs approximately half the leeway angle at equal side force as compared with models 3 and 7. Both nrs. 3 and 7 have a large beam-draught ratio. A good deal of the difference is due to the zero side force leeway angle, which is large for the hulls with a large beam-draught ratio. Apparently the large B_{WL}/T_c hull has a larger asymmetry when heeling. The corresponding side force due to the hull is directed to the leeside of the yacht in all of the considered cases. Figure 10 shows that the slope of the lines $\frac{d(F_H \cos \phi)}{d\beta}$ increases with increasing draught of the canoe body. The data indicate that in the considered range of leeway angles a linear relation between side force and leeway angle exists at constant forward speed and heel angle. Within practical limits, the side force varies as V^2 at constant leeway and heel angle, as suggested by Kerwin [13].

Measurements of side force and resistance at various leeway angles but zero heel are carried out for all nine models at speeds corresponding to Froude numbers of 0.20 and 0.35. Although in the ocean sailing practice side force is commonly associated with both leeway and heel, these tests may provide useful basic information on side force production. A plot of measured side force versus leeway angle represents the lift curve of the complete underwaterbody. Its slope in the origin, which indicates the effectiveness of side force production, is given for all nine models in Table 4. The values are made non-dimensional by dividing by $\frac{1}{2}\rho V^2 L_{WL}{}^2$. In confirmation of the statements above the most effective side force production, e.g. the steepest side force curve, may be expected with the deepest draughts. The slight speed dependency is caused by the corresponding generated wave systems. In Table 4 the experimental values are compared with calculations according to a method introduced by Gerritsma [16]. This method is valid for fin keel and rudder yachts and is based on a virtual extension of keel and rudder to the waterline as shown in Figure 11, after which aerodynamic theories may be applied on both fins. The extensions are assumed to represent the contribution of the hull. A graphical comparison of experimental

Table 4
Calculated and measured side force curve slope

Nr	T m	$Y'_\beta \times 10^5$		
		measured		calculated
		$F_n = .20$	$F_n = .35$	
1	2.16	12400	12400	12630
2	2.28	12700	12800	13654
3	2.05	11800	12300	11618
4	2.09	11400	11600	11962
5	2.28	13000	13600	13688
6	2.43	14500	15500	15118
7	2.01	10800	11200	11260
8	2.16	12800	13600	12630
9	2.16	12450	13150	12630

$$Y'_\beta = \frac{dF_H}{d\beta} / \tfrac{1}{2}\rho V^2 L_{WL}{}^2$$

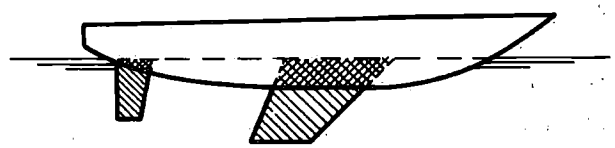

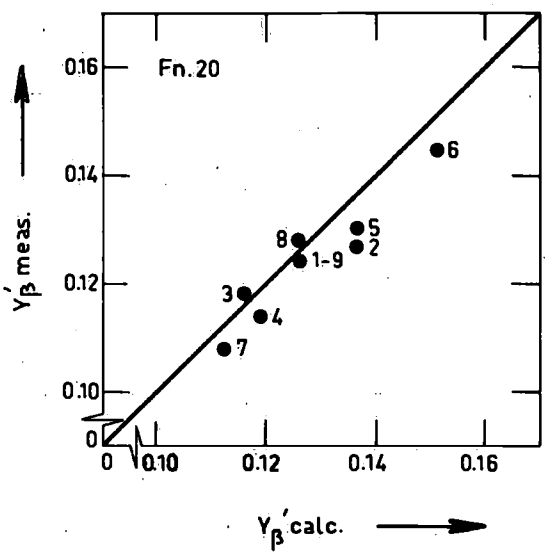

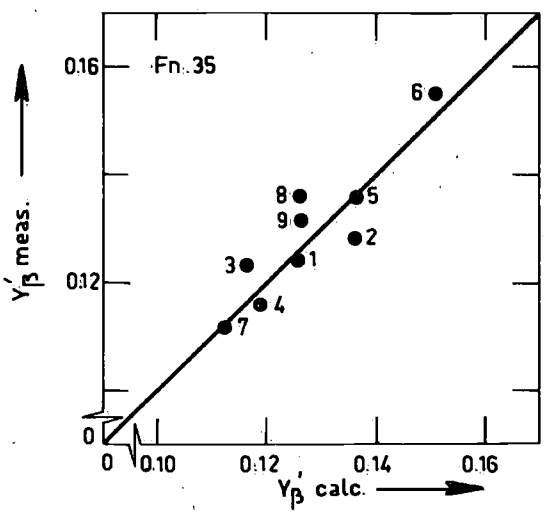

Figure 11. Calculated and measured side force curve slopes.

and calculated values in Figure 11 shows that the method gives useful predictions. The root mean square relative error of the prediction is 4.4% and 4.5% for Froude number .20 and .35 respectively.

3.4. Heeled and induced resistance

In addition to the upright condition, a sailing yacht experiences an extra resistance force due to heel and side force. This resistance component is important as shown by the analysis of model test data. For instance at the maximum attainable close-hauled yachtspeed (approximately: $F_n = 0.35$) the frictional-, residuary- and heeled + induced resistance are roughly equal in magnitude. On other courses and forward speeds the relative importance of the various resistance components is different. The heeled resistance can be defined as the extra resistance at zero side force, although as shown in Figure 10, this condition requires a leeway angle to counteract the side force produced by the asymmetrical immersed part of the hull. Following this definition the heeled resistance and the resistance induced by the side force can be distinguished in Figure 12 for the case of a thirty degrees heel angle with:

$$R_\phi - R_T = R_H + R_i \qquad (9)$$

where:

R_ϕ - total resistance with heel and leeway angle
R_T - total resistance in upright position
R_H - heeled resistance at zero side force
R_i - induced resistance due to leeway.

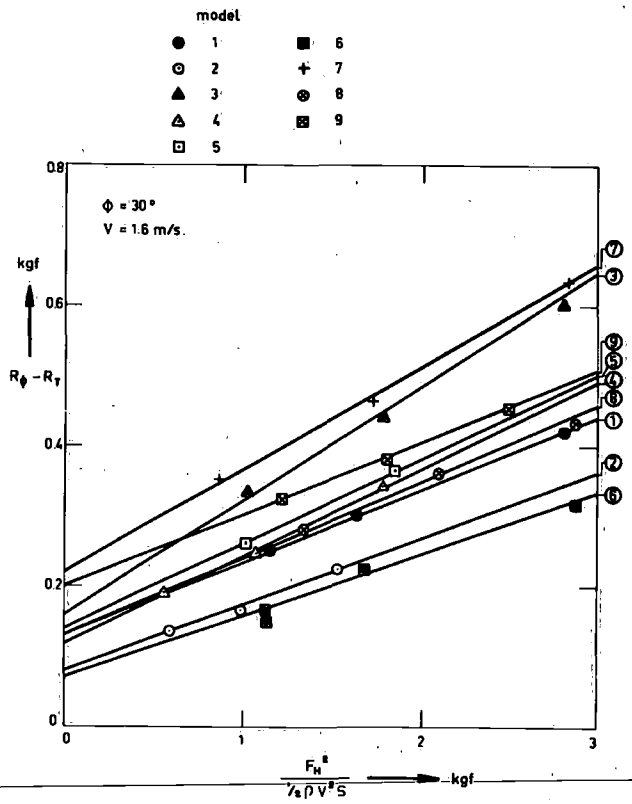

Figure 12. Heeled and induced resistance.

The highest values for the heeled and induced resistance are found for models 3 and 7 (both shallow hull forms) and the lowest values correspond with the largest draught (model 6). The differences between the highest and the lowest values are significant in the considered case ($\phi = 30°$, V = 1.6 m/s, model value). Apparently this is due to the differences in the effective aspect ratio of the combination of keel + rudder + underwater part of the hull, which varies from model to model due to variations in hull form. From airfoil theory the following relation between the induced resistance and the lift is known:

$$C_{D_i} = \frac{C_L^2}{\pi AR_E} \qquad (10)$$

where: AR_E - the effective aspect ratio of the wing. For the present purpose this can be written as:

$$R_i = \frac{F_H^2}{\frac{1}{2}\rho V^2 S \times C} \cdot f(\phi) \qquad (11)$$

where: S - the total wetted surface or a representative area of hull, keel and rudder combination. In [13] Kerwin suggested for $f(\phi)$:

$$f(\phi) = C_1 + C_2 \phi^2 \qquad (12)$$

where C_1 and C_2 are constant to be determined from the experiments. To show the relation between the heeled and induced resistance versus side force as indicated by equations (9) and (11), the extra resistance $R_\phi - R_T$ is plotted on a base of $F_H^2/\frac{1}{2}\rho V^2 S$ in Figure 12.

4. Sailing performance

4.1. Determination of sailplan and stability

To predict sailing performance stability and sailplan must be determined for each model in a systematic way and matched consistently to the given hull dimensions. The following method has been chosen:

a) Hull weights, including crew and equipment, are calculated with

$$W_H = C_H . L . B_{MAX} . D$$

where:

C_H is a constant, for which a value of 65 represents current consturction methods, materials and crew size.

L is length in m, taken as the average of overall length and waterline length (respectively 12.65 m and 10.00 m for all models).

B_{MAX} is maximum breadth.

D_H is depth of the hull, which equals the constant freeboard (1.15 m) plus the draught of the canoe body.

The centre of gravity of hull weight (including crew) is assumed to be at 80% of the depth above the base line and in the centre plane of the ship. So in the stability calculations no allowance is made for asymmetric crew positions.

b) The available weight for ballast is obtained by subtracting the estimated hull weight from the given weight of displacement. It is cast as lead into the keel, assuming a specific weight of 11000 kg/m^3. Thus it fills up to a certain height and gives the position of the centre of gravity of ballast.

c) The position of the total centre of gravity is obtained by adding hull and ballast parts. Stability moments are calculated;

d) Basic proportions of the sailplan as indicated in Figure 13 are assumed. Though these assumptions are in fact arbitrary they reflect the actual design practice on a base of IOR regulations and may thus represent common yachts.

e) Maintaining the proportions mentioned under d the mast height is varied in such a way that the ratio of heeling moment to stability moment at 30° heel is equal for all ships. This ratio is represented by:

$$SR = \frac{SA.h}{(RM)_{\phi=30°}} \qquad (13)$$

with:

$SA = \frac{1}{2} I.J + \frac{1}{2}.P.E$

$h = Z_{CE} + 0.4 \cdot T_T$

where:

SA : represents sail area to windward

h : represents the arm of heeling moment.

I, J, P, E are sail dimensions according to Figure 13.

Z_{CE} : height centre of effort of sail area SA above the waterline

T_T : total draught.

For the present analysis the value of SR has been chosen as 10. The heel angle of 30° has been selected because this value is often encountered in conditions where stability becomes an important factor to performance.

Results of the above calculations are shown in Table 5 for weight and stability and in Table 6 for sail dimensions and derived parameters. The resulting ballast ratios (Table 5) have normal values. The position of the centre of gravity is in some cases probably a bit low compared to normal practice. This may be caused by the wide variations in total draught, due to the use of a standard keel under different hull shapes. This is contrary to the standard total draught stimulated by the IOR. The obtained sailplans have normal dimensions. It must be noted that the effective sail areas downwind and to windward, as given in Table 6, are calculated different from the area SA used above, though they are linearly related to SA. The downwind area SA_{ed} consists of mainsail and spinnaker and is estimated as:

$$SA_{ed} = 1.4.I.J. + \frac{1}{2}.P.(E + HB) \qquad (14)$$

where:

HB = standard breadth of mainsail headboard.

The sail area to windward consists of mainsail area, neglecting roach, plus the area of a standard IOR 150% genoa. Although height and area of the rigs are selected in a fixed relation to stability moment, the sail area to wetted area and sail area to displacement ratios still vary considerably. The light models 4 and 7, with low

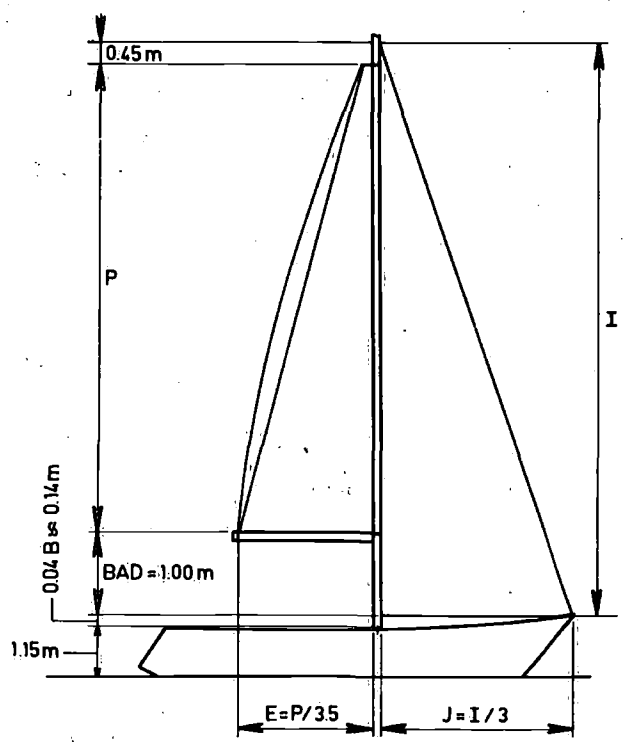

Figure 13. Standard sail plan design.

Table 5
Weight and stability data

Nr	BR %	Z_G m	$\overline{GM}$ m	RM at $\phi = 1°$ kgm	RM at $\phi = 30°$ kgm
1	47	−0.34	1.30	224	6095
2	51	−0.48	1.00	173	4915
3	42	−0.19	1.90	327	7873
4	44	−0.29	1.12	161	4376
5	49	−0.40	1.54	343	9492
6	54	−0.56	1.14	256	7026
7	40	−0.15	1.45	204	4682
8	49	−0.38	1.32	227	6223
9	45	−0.30	1.29	222	5966

BR = Ballast Ratio

Table 6
Sail dimensions

Nr	I m	J m	P m	E m	SA_{ed} m^2	SA_{eb} m^2	Z_{CE} m	$\frac{(SA_{ed})^{1/2}}{S}$ *	$\frac{SA_{ed}^{1/2}}{\nabla^{1/3}}$ *
1	16.47	5.49	15.02	4.29	159.8	104.7	6.99	2.18	5.89
2	15.23	5.08	13.78	3.94	136.3	89.1	6.56	2.06	5.44
3	18.07	6.02	16.62	4.75	192.9	126.7	7.55	2.32	6.48
4	14.64	4.88	13.19	3.77	125.6	82.1	6.36	2.01	5.55
5	19.24	6.41	17.79	5.08	219.2	144.0	7.95	2.43	6.33
6	17.27	5.76	15.82	4.52	176.1	115.5	7.26	2.22	5.65
7	15.02	5.01	13.57	3.88	132.5	86.6	6.50	2.03	5.74
8	16.61	5.54	15.16	4.33	162.6	106.6	7.04	2.20	5.94
9	16.34	5.45	14.89	4.25	157.3	103.0	6.95	2.18	5.84

*) The ratios of windward sail area to wetted area and displacement are proportional to the downwind sail area ratios.

Table 7
Rating parameters

Nr	MR m	R ft	TMF
1	10.62	34.2	1.0646
2	10.05	33.2	1.0528
3	11.40	36.7	1.0930
4	10.09	32.5	1.0443
5	11.17	36.3	1.0886
6	10.48	34.9	1.0727
7	10.30	32.9	1.0492
8	10.73	35.6	1.0807
9	10.33	33.1	1.0516

ballast ratios and according low positions of the centre of gravity, have a small sail area compared to wetted area. A low stability moment due to a small breadth, like with model 2, resulsts also in a relatively undercanvassed boat. Contrary, a wide hull, when combined with a normal or heavy displacement, like models 3 and 5 results in relatively large rigs.

Finally the rating of the resulting designs has been calculated, assuming an equal engine weight and position and equal propeller dimensions and immersion. From Table 7 it appears that the rating of this series covers a margin of abt 4 feet, which is appreciable for ships with equal length.

4.2. Downwind speed

The downwind speed is calculated from the upright resistance tests, assuming a drag coefficient for the sails of 1.2. Furthermore it is assumed that sailing down-

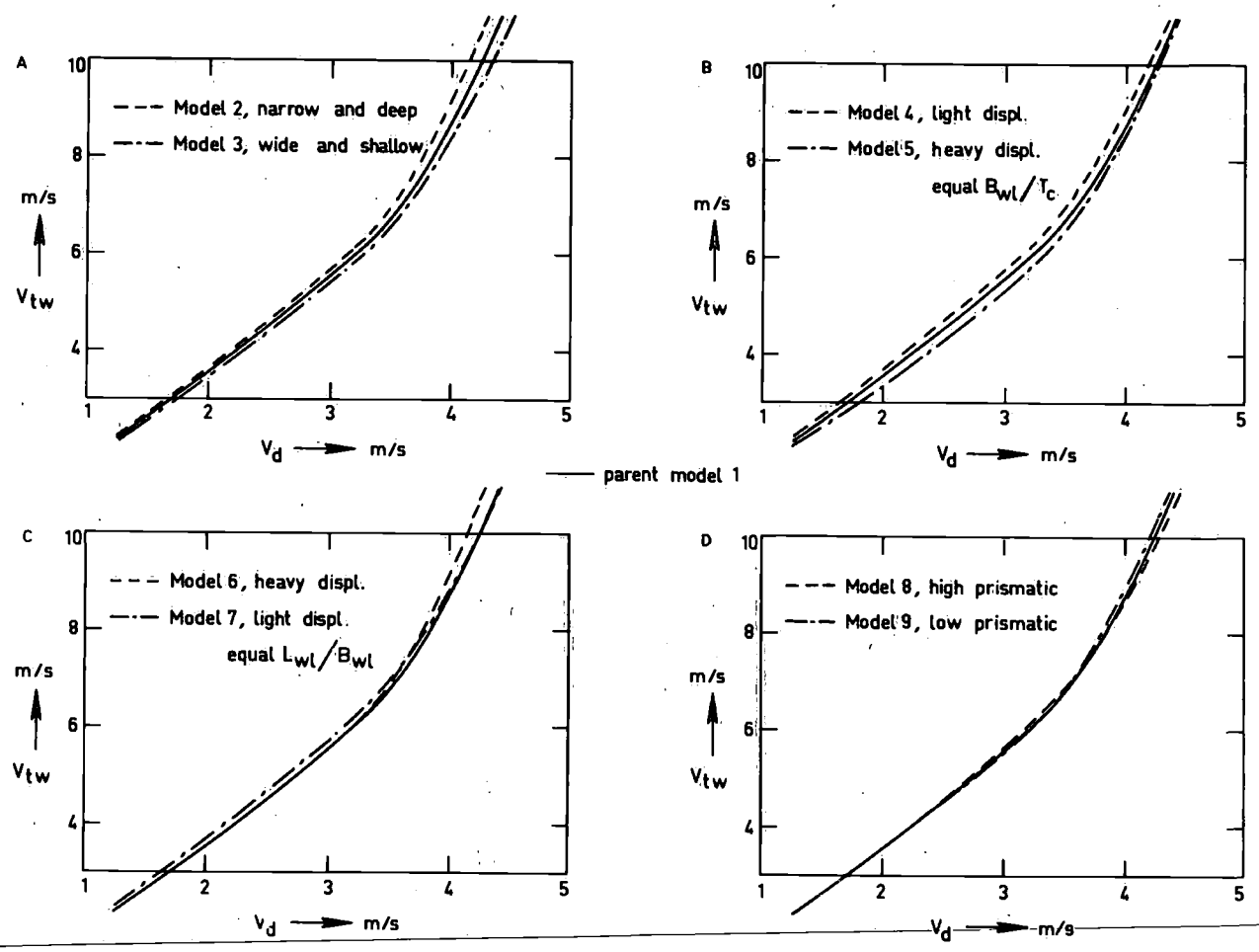

Figure 14. Downwind speed.

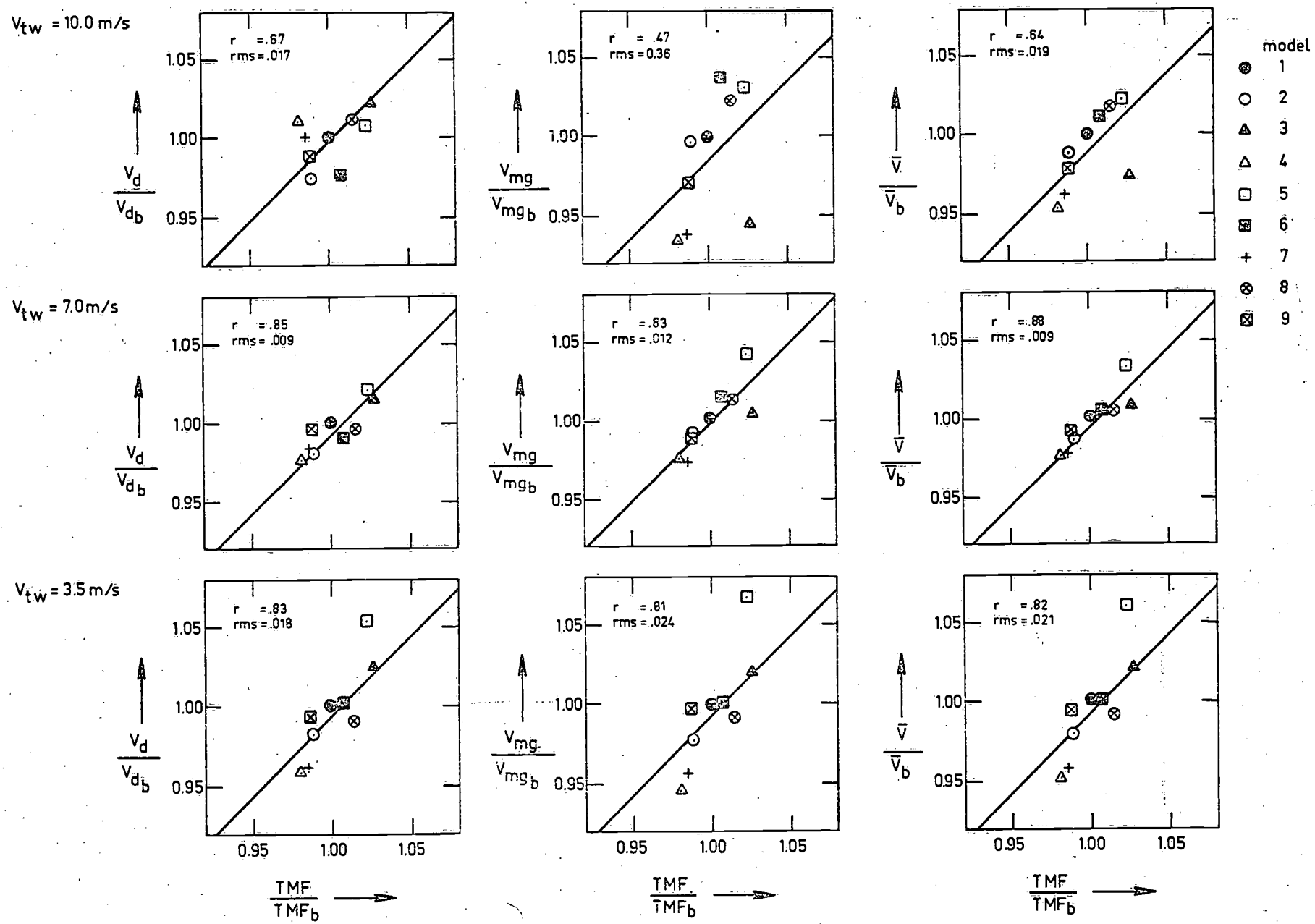

Fig.16: Downwind, made-good and average speed related to rating. (L_{wl} = 10 m)

wind does not give heel and does not necessitate a rudder angle. The results are given in Figure 14. To show the additional influence of sail area above the resistance as shown in Figure 8, the different models are grouped in the same way.

While the resistance of models 1, 2 and 3 (Figure 8a) is nearly equal, the downwind speed differs greatly due to the difference in sail area. As said before model 2 has less sail area because its narrow beam and according low initial stability does not permit to carry more sail to windward. The beamy model 3 is just the opposite.

A comparison of models 1,4 and 5 shows again the important effect of sail area. Though the light displacement model 4 has less resistance than 1 and 5, its downwind speed is still lower than the others because its more strongly reduced sail area.

According to Figure 14c the difference in resistance between models 1,6 and 7, as observed in Figure 8c is apparently better compensated by sail area than the foregoing combinations. The improving performance of the light displacement yacht with increasing wind speed, and the reversed characteristics of the heavy boat may be noted.

As shown in Figures 8d and 14d the influence of prismatic coefficient is of second order, at least if otherwise hull dimensions and displacement are comparable.

However, the slightly favourable effect of a high prismatic at higher boat speed and wind velocity is noticeable from both Figures.

If downwind speed as related to resistance is compared with the sail area - wetted area and sail area - displacement ratios from Table 6, it may be concluded that high ratio values favour the downwind performance. As may be obvious the sail area-wetted area ratio greatly governs the lower wind speed range, while the sail area - displacement ratio may indicate the downwind speed at higher wind speeds.

4.3. Speed-made-good to windward

The speed-made-good to windward of all 9 models is calculated according to Davidson's method [1], using the Gimcrack sail coefficients. However, as a result of recent investigations [13] the Gimcrack coefficients are applied to the geometric area of main sail and genoa, including overlap, instead of the reduced effective area proposed by Davidson. This modification takes into account the improvements in sail cloth and rig design during the last decades and gives a better prediction of heeling angle without affecting the qualities of Davidson's method. The results of the calculations are shown in Figure 15, arranged conform Figures 8 and 14. The influence of sail area and stability on windward performance above that of hydrodynamic resistance and side force properties may be indicated by comparing these figures.

Figure 15a presents the characteristic differences between speed-made-good curves of a narrow and deep respectively wide and shallow hull. At lower wind speeds, if only a moderate side force production is required, resistance and driving force characteristics are dominant. So in this case the beamy model 3 with its large sail area attains the highest speeds, both to windward and downwind. The narrow model 2 may still be considered as undercanvassed in these conditions. When wind speed increases the balance between stability and heeling moment and the efficiency of side force production becomes more important. As discussed in paragraphs 3.3 and 3.4 the deep draught model 2 requires smaller leeway angles to generate a prescribed side force (Figure 10c) than the shallow model 3, and does this with much less resistance increase (Figure 11). From these hydrodynamic characteristics it may be expected that at high wind speeds model 2 is better than model 3 as shown in Figure 15a. In the case of extreme wide and shallow hulls large drops in windward performance may occur with increasing wind speed and heel angle. With respect to models 2 and 3 it must be remarked that in practical designs model 2 should be equipped with a somewhat smaller keel, to reduce wetted area and model 3 with a more extended keel, to improve side force production.

Figure 15b demonstrates that the differences which models 4 and 5 in downwind conditions are likely retained when sailing to windward. This must be largely due to maintaining a constant breadth-draught ratio when varying displacement. This results in a comparitively low stability for the light model 4, combined with a relatively low sail area as a consequence of the design rules given in paragraph 4.1. The heavy model 5 has just opposite characteristics. Besides, the shallow draught of the light model 4 results in relatively poor side force and induced resistance properties (see paragraphs 3.3 and 3.4) and will therefore adversely affect the speed-made-good curve at high wind velocities. In practical designs the light displacement of model 4 might have been obtained with a somewhat wider hull and combined with a deeper keel and slightly larger sail plan.

An analysis of the differences between models 1, 6 and 7 is probably more speculative. Though the beam of model 6 should expect a sufficiently large sail area, this is apparently not enough if related to wetted area, to obtain a light weather performance which is equivalent to models 1 and 7. The relatively worsening qualities of model 6 and the improving qualities of model

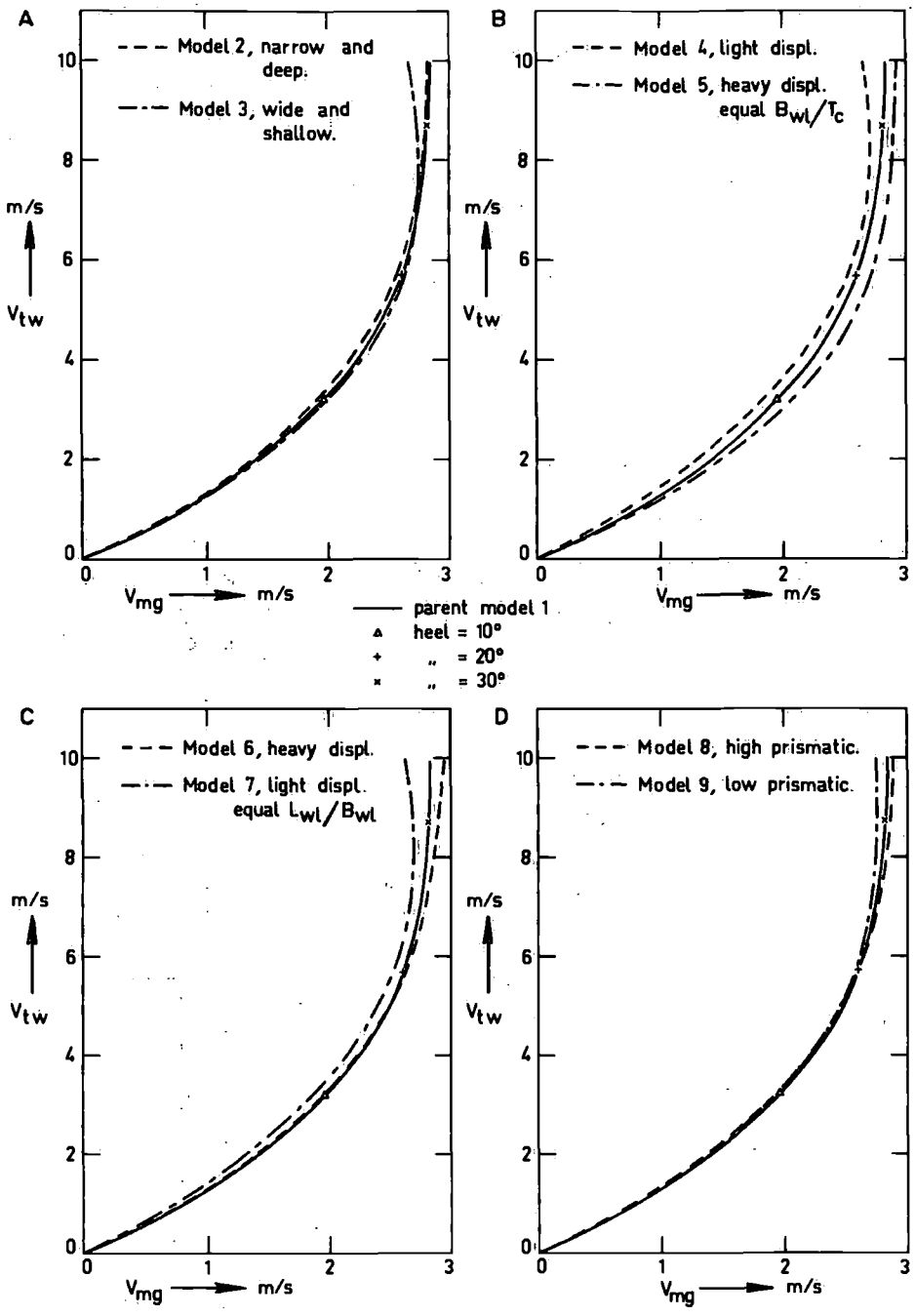

Figure 15. Speed-made-good to windward.

7 at true wind speeds near 9 m/s might be attributed to the shallow respectively deep draught and consequently worse and better efficiency of side force production. As can be seen from Figures 10c and 12 the light, shallow draught model 7 operates at very high leeway angles and gives an appreciable resistance increase due to heel and leeway, whereas the deep model 6 demonstrates good properties within this respect.

The influence of prismatic coefficient, with otherwise comparable hull dimensions and sail plan is also demonstrated in the windward performance of models 8 and 9. In the high wind speed and consequently high boat speed range. the high prismatic model 8 shows advantages above the low prismatic model 9. This phenomenon does completely agree with the resistance curves (Figures 8d) and downwind speed (Figure 14d).

As a general conclusion it may be stated that a high sail area - wetted area ratio works advantageous in light weather, whereas at higher wind speeds a deep keel and right balance between stability moment and sail area might improve the performance to windward.

4.4. Performance with respect to rating

For racing yachts the attainable speeds have to be

related to a predetermined handicap. In most European ocean races during the 1976 and 1977 seasons the handicap consisted of multiplicating the elapsed time with a TMF (Time Multiplication Factor), which was based as follows on the IOR-rating [17].

$$TMF = \frac{A\sqrt{R}}{1 + B\sqrt{R}}$$

where:

R = rating in feet

A = 0.2424] for yachts with rating
B = 0.0567] above 23 feet (class I - IV)

or:

A = 0.4039] for yachts with rating
B = 0.2337] under 23 feet (class V - VIII)

Rating R and TMF are calculated for all 9 models and given in Table 7. The rating formula intends to give an estimate of the yacht's speed potential, whereas the handicap system is constructed in such a way that the derived TMF ought to be directly proportional to speed. Figure 16 shows the speed at standard true wind speeds of 3.5, 7.0 and 10.0 m/s versus TMF, where model 1 has been used as base boat, with suffix b. Speed is distinguished in downwind speed, speed-made-good to windward and the average speed on a standard track parallel to the wind direction, which has to be sailed to windward and downwind. Based on the assumption that speed and TMF should be proportional to each other, lines have been drawn through the points with the aid of the least squares fit. The root mean square of the deviation of all points with respect to this line is also shown in Figure 16 with rms. Secondly the correlation coefficient of all speed-TMF combinations is determined, based on an assumed linear relationship. The results are for all sailing conditions given in Figure 16 under r. If it is realised that the standard way in which hull forms, keel-rudder arrangements, stability and sail plans of this series are determined might give deviations from optimal designs, and if it is furthermore realised that it is impossible to set one single handicap being equally fair in all sailing conditions, the IOR-rating system seems to be a surprisingly good speed estimator. A root mean square error of the speed prediction which is less than 2% in most conditions may be considered very satisfactory from an engineering point of view. Yet, racing sailors will require even less "probability" in their competition results. From Figure 16 it appears that the IOR is especially aimed at average wind conditions, represented by the 7 m/s wind velocity. Downwind speed seems to be better predicted than speed-made-good to windward. This indicates that the IOR rates fairly well the upright hull with according resistance and the downwind sail area, but has problems in discovering all

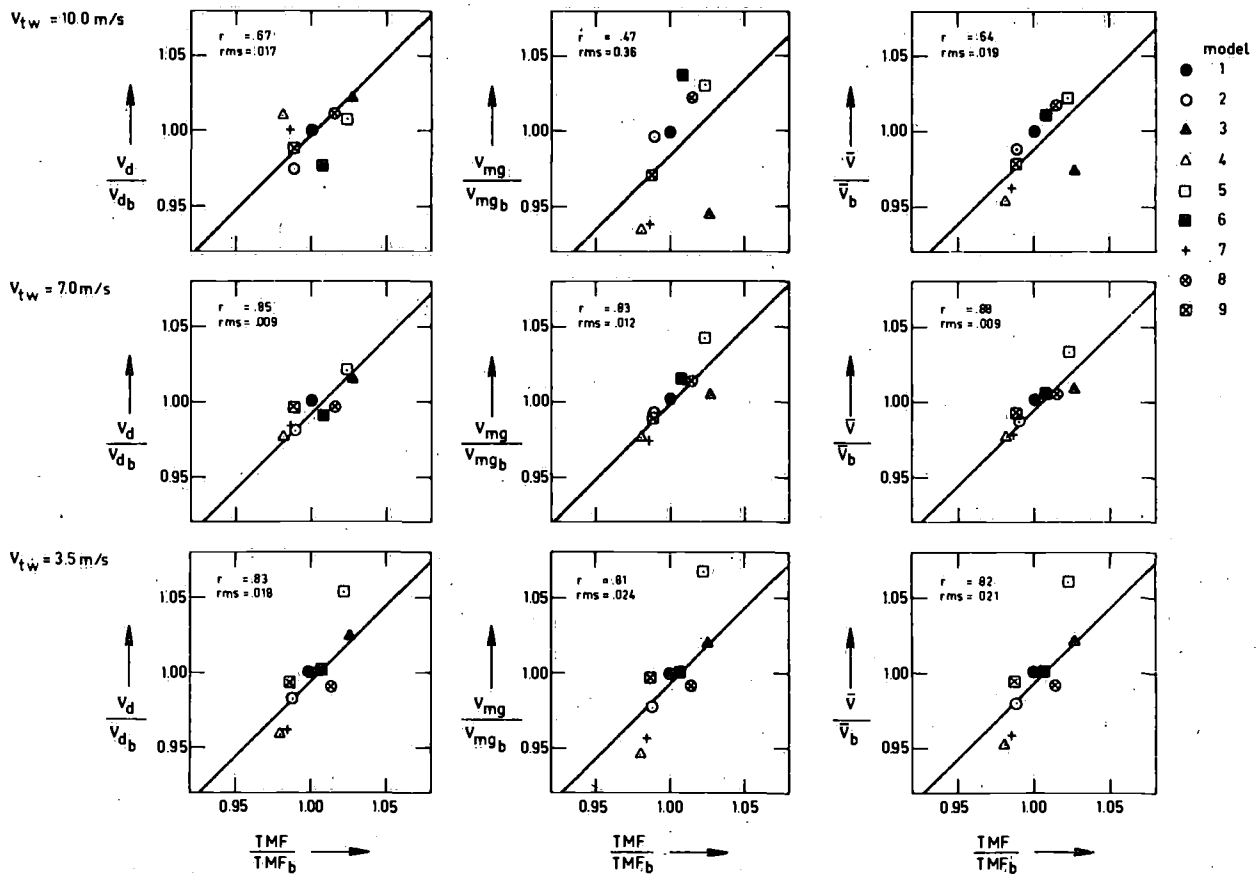

Figure 16. Downwind, made-good and average speed related to rating.

significant effects of stability and the keel-rudder configuration, when going to windward. It will indeed be difficult to imply these effects in one single formula. All statements and conclusions above are based on calculations with yachts of equal hull length, but further strongly varying parameters. Further calculations with length as additional variable may necessitate a revision of the TMF-formula with respect to its proportionality to speed for a wider length range, but will otherwise probably confirm the conclusions above.

5. Acknowledgement

The authors want to mention the good and fruitful cooperation with Professor J.E.Kerwin, Professor J.N. Newman and O.H. Oakley, with the Massachusetts Insitute of Technology at Boston, who contributed to a great deal to the succes of the reported series. Further, they are indebted to Frans Maas, Breskens, for permission to use his design as parent model, and E.G. van de Stadt & Partners for their practical advices in consistently determining stability and sail plan. Finally, thanks to Mrs. Joke de Jager and Piet de Heer for carefully typing this manuscript and drawing the figures.

References

1. Davidson, K.S.M., "Some experimental studies of the sailing yacht", Society of Naval Architects and Marine Engineers, N.Y., 1936.
2. Taylor, D.W., "The speed and power of ships", Washington, 1933.
3. Saix, P. de, "Systematic model series in the design of the sailing yacht hull", 2nd HISWA Symposium, 1971, Amsterdam.
4. Gerritsma, J. and Moeyes, G., "The seakeeping performance and steering properties of sailing yachts", 3rd HISWA Symposium, 1973, Amsterdam.
5. Saix, P. de, "Fin-hull interaction of a sailing yacht model", SIT, DL, Technical Memorandum 129, 1962.
6. Millward, A., "The design of spade rudders for yachts", University of Southampton, Report 28, 1969.
7. Herreshoff, H.C. and Kerwin, J.E., "Sailing yacht keels", 3rd HISWA Symposium, 1973, Amsterdam.
8. Beukelsman, W. and Keuning, J.A., "The influence of fin keel sweep back on the performance of sailing yachts", 3rd HISWA Symposium, 1973, Amsterdam.
9. Marchaj, C., "Wind tunnel tests of a ¼ scale dragon rig", University of Southampton, Dept. of Aeronautics, SUYR Paper no. 14, 1964.
10. Herreshoff, H.C., "Hydrodynamics and aerodynamics of the sailing yacht", Society of Naval Architects and Marine Engineers, 1964.
11. Wagner, B. and Boese, P., "Windkanal Untersuchungen einer Segelyacht", Schiff und Hafen, 1968.
12. Kerwin, J.E., Oppenheim, B.W. and Mays, J.H., "A procedure for sailing performance analysis based on full scale log entries and towing tank data", M.I.T. Report no. 74-17, 1974.
13. Gerritsma, J., Moeyes, G. and Kerwin, J.E., "Determination of sail forces based on full scale measurements and model tests", 4th HISWA Symposium, 1975, Amsterdam.
14. "Principles of Naval Architecture", Editor J.P. Comstock, N.Y., 1967.
15. Milgram, J.H., "Sail force coefficients for systematic rig variations", SNAME Technical & Research Report R-10, 1971.
16. Gerritsma, J., "Course keeping qualities and motions in waves of a sailing yacht", 3rd AIAA Symposium on the Aero/hydrodynamics of sailing, California, 1971; also: Delft Ship Hydromechanics Laboratory, Report 200, 1968.
17. "International Offshore Rule IOR Mark III", Offshore Rating Council, IYRU.

List of symbols

A_w	waterplane area
A_x	maximum sectional area
AR_E	effective aspect ratio
B	centre of buoyancy
B_{MAX}	maximum breadth
B_{WL}	waterline breadth
BAD	height of boom above deck
$\overline{BM}$	metacentric radius
$\overline{C}$	average chord
C_{D_i}	induced drag coefficient
C_F	frictional resistance coefficient
C_H	weight coefficient of hull
C_L	lift coefficient
C_P	prismatic coefficient
D	depth
E	length of main sail foot
F	freeboard
F_n	Froude number
F_H	heeling component of sail force
G	centre of gravity
g	gravity acceleration
$\overline{GM}$	metacentric height
$\overline{GN} \sin \phi$	arm of static stability
h	height of centre of effort of sails above waterline
HB	breadth of main sail headboard
I	foretriangle height
I_L	longitudinal moment of inertia of waterplane
I_T	transverse moment of inertia of waterplane
J	length of foretriangle base
K	keel point
$k(\phi)$	dimensionless residuary stability
$\overline{KB}$	height of centre of buoyancy above base line
$\overline{KM}$	height of metacentre above base line
L	length
L_{OA}	length over all
L_{WL}	waterline length
LCB	longitudinal position centre of buoyancy
LCF	longitudinal position centre of flotation

M	metacentre
$\overline{MN} \sin \phi$	arm of residuary stability
MR	measured rating
P	length of main sail luff
R	rating
R_F	frictional resistance
R_H	heeled resistance at zero side force
R_i	induced resistance due to leeway
R_n	Reynolds number
R_R	residuary resistance
R_T	total resistance in upright position
R_ϕ	total resistance with heel and leeway
RM	righting moment
S	wetted area
SA	sail area
SA_{eb}	effective sail area to windward
SA_{ed}	effective sail area downwind
SR	stability ratio
T	draught
TMF	time multiplication factor
V	speed
V_d	downwind speed
V_{mg}	speed-made-good to windward
V_{tw}	true wind speed
W_H	hull weight
Y'_β	sideforce curve slope, made dimensionless by $\frac{1}{2}\rho V^2 L_{WL}{}^2$
Z_{CE}	height of effective centre of effort of sail force above waterline
a	linear scale ratio
β	leeway angle
Δ	weight of displacement
∇	volume of displacement
ϕ	heeling angle
γ	kinematic viscosity
ρ	specific density

Subscripts:

b	refers to base boat
c	refers to canoe body
k	refers to keel
r	refers to rudder